Universidade de Aveiro Departamento de Ciências Médicas
2018

FLÁVIA SOFIA RODRIGUES DE ALMEIDA PASCOAL

O PAPEL DA CDC42 NA MIGRAÇÃO CELULAR MEDIADA POR APP

CDC42 ROLE IN APP-MEDIATED CELL MIGRATION

Universidade de Aveiro Departamento de Ciências Médicas
2018

FLÁVIA SOFIA RODRIGUES DE ALMEIDA PASCOAL

O PAPEL DA CDC42 NA MIGRAÇÃO CELULAR MEDIADA POR APP

CDC42 ROLE IN APP-MEDIATED CELL MIGRATION

Dissertação apresentada à Universidade de Aveiro para cumprimento dos requisitos necessários à obtenção do grau de Mestre em Biomedicina Molecular, realizada sob a orientação científica da Doutora Sandra Isabel Vieira, Professora Auxiliar Convidada do Departamento de Ciências Médicas da Universidade de Aveiro

Este trabalho contou com o apoio do Instituto de Biomedicina (iBiMED, UID/BIM/04501/2013) e do projeto GoBack - Novos alvos terapêuticos para a lesão medular (PTDC/CVT-CVT/32261/2017)

Dedico este trabalho aos meus pais e amigos por todo o apoio.

o júri

presidente

Professora Doutora Margarida Sâncio da Cruz Fardilha
Professora Auxiliar C/ Agregação, Departamento de Ciências Médicas da Universidade de Aveiro

Professora Doutora Sandra Isabel Moreira Pinto Vieira
Professora auxiliar convidada, Departamento de Ciências Médicas da Universidade de Aveiro

Doutora Ana Sofia da Cunha Guimarães
Investigadora de Pós-doutoramento do Instituto de Biologia Molecular e Celular, Instituto de Investigação e Inovação em Saúde (I3S) da Universidade do Porto

agradecimentos

À minha orientadora, Sandra Vieira, por todo o apoio durante a realização deste trabalho, e pelos conhecimentos transmitidos

À Doutora Maria Lázaro, pela preciosa ajuda e disponibilidade em colaborar na análise por FRAP

Ao Doutor André Maia pela ajuda disponibilizada na utilização do software ImageJ e pela colaboração no ensaio de SWH

À Mariana Alves pelo apoio na utilização da LiM facility of iBiMED, um nó da PPBI (Portuguese Platform of BioImaging): POCI-01-0145-FEDER-022122

Aos meus pais que me incentivaram ao longo de todo o meu percurso académico e o tornaram possível

À Patrícia, à Bárbara e ao Roberto, pela ajuda disponibilizada sempre que precisei

Ao Hugo, que nunca desistiu de me incentivar nos momentos mais difíceis

Aos meus amigos que sempre se mantiveram do meu lado e me apoiaram durante todo o processo

Às minhas grandes companheiras e amigas de Mestrado, Ana Teixeira, Beatriz Silva, Cláudia Ribeiro e Bárbara Morgado, pelos 2 anos de amizade, companheirismo e boa disposição e por terem partilhado comigo todos os momentos bons e maus, e todo o processo desta tese, tornando o último ano muito mais fácil de passar

palavras-chave

APP, Cdc42, Migração celular, Direção de migração, Fenótipo Migratório, F-Actina.

resumo

A migração celular é transversal a vários processos celulares como embriogénese, metástase, resposta imunitária e regeneração. A proteína precursora de amilóide de Alzheimer (APP) e a proteína GTPAse Cdc42 têm sido, separadamente, associadas a vários processos relacionados com migração celular, nomeadamente: velocidade, a polarização das células, e o desenvolvimento de estruturas migratórias como filopódias e lamelopódias. Neste trabalho pretendíamos confirmar o papel da APP na persistência na direção de migração de células de tipo neuronal, previamente observado pelo nosso grupo, e averiguar se a APP interagia com a Cdc42 neste mesmo processo. Para tal realizaram-se estudos de biologia celular em células SH-SY5Y transfetadas com cDNAs de APP-GFP e DsRed-Cdc42 (wt ou dominant negative, DN) e recorreu-se à técnica de "Scratch Wound Healing" que permite estudar vários parâmetros migratórios. A migração das células foi monitorizada hora a hora durante 13 horas por microscopia de fluorescência e o percurso, a distância e a velocidade de migração analisados com a ajuda do software Image J. Através de ensaios de imunocitoquímica analisámos o efeito destas duas proteínas na morfologia das células. Por último, estudámos a influência da APP na dinâmica da F-actina em células SH-SY5Y, comparando com dados prévios do nosso grupo para células não neuronais. Para tal recorreu-se à técnica de FRAP para análise "in vivo" de células que co-expressavam GFP ou APP-GFP, e um marcador fluorescente de F-actina (LifeAct-RFP).
Os resultados obtidos confirmaram que a APP aumenta a persistência na direção de migração em células SH-SY5Y, mas que este aumento deixa de ocorrer quando se sobre-expressa a APP conjuntamente com Cdc42 wt. No entanto, quando há sobre-expressão de APP com Cdc42 DN, a migração volta a um padrão mais direcionado, o que leva a crer que a APP não aumenta o direcionamento das células via ativação da Cdc42. Por outro lado, a presença de APP diminui ambos os parâmetros distância total e a velocidade de migração das células, em relação ao controlo GFP, e a presença de Cdc2 wt potenciou esse efeito. Neste caso, a inibição da atividade da Cdc42 anulou o efeito da APP, sendo que as células voltaram a exibir valores de distância e velocidade semelhantes às células controlo. No que toca à aquisição de fenótipo migratório, a APP não teve grande influência neste, ao contrário de ambas as Cdc42 (wt e DN), que aumentaram a percentagem de células com fenótipo migratório, confirmando que a molécula da Cdc42 por si só é importante para a polarização das células. Por último, observámos que a APP parece favorecer a dinâmica da F-actina. Estes resultados contribuem para a compreensão dos mecanismos subjacentes ao papel da APP e da Cdc42, e sua interacção funcional, em processos de migração de células do tipo neuronal.

keywords

APP, Cdc42, Cell Migration, Direction of migration, Migratory Phenotype, F-actin.

abstract

Cellular migration is transversal to several cellular processes such as embryogenesis, metastasis, immune response and regeneration. The amyloid precursor protein and the Cdc42 protein have been separately associated with several processes related to cell migration, namely: velocity, cell adhesion, cell polarization, and the development of migratory structures such as filopodia and lamellipodia. In this work we intended to confirm the role of APP in persistent direction of migration of neuronal-like cells, previously observed in our group, and to investigate if APP interacted with Cdc42 in this same process. Cell biology studies were carried out on SH-SY5Y cells transfected with APP-GFP and DsRed-Cdc42 (wt ou dominant negative, DN) cDNAs, and a Scratch Wound Healing assay was used to study cell migration parameters. Cells migration was monitored hourly for 13 hours by microscopy means, and the path, distance and velocity of the cells were analyzed with the help of the Image J software. We also analyzed the effects of these two proteins on the cell morphology using immunocytochemistry assays. Finally, we intended to study the influence of APP on the dynamics of F-actin in neuronal-like cells, to compare with our previous results in non-neuronal cells. For this we resorted to a FRAP analysis of live cells co-expressing APP-GFP and LifeAct-RFP, a fluorescent marker of F-actin.

The results confirmed that APP positively influences persistence in the migration direction of SH-SY5Y cells. However, when co-expressed with Cdc42 wt the cells no longer migrated in a targeted manner. When Cdc42 was overexpressed but its catalytic activity inhibited (Cdc42 DN), the migration returned to a more directed pattern, which leads us to believe that APP does not increase persistence in the migration direction via Cdc42 activation. On the other hand, the presence of APP decreases both parameters of total migrated distance and the cells' migration velocity in relation to the control GFP, and the presence of Cdc2 wt further decreased these values. In this case, inhibition of Cdc42 activity annulled APP effect, and cells returned to distance and velocity values similar to control cells. Regarding the acquisition of migratory phenotype, APP showed litle influence, unlike both Cdc42 (Wt and DN) that increased the percentage of cells with this phenotype, proving that the Cdc42 molecule alone is important for the cells polarization. Finally, we observed that APP tended to promote the dynamics of F-actin. These results contributed to better understand the mechanisms underlying the role of APP and Cdc42, and their functional interaction, in migration processes of neuronal-like cells.

List of contents

List of Figures

List of Abbreviations

APP	Alzheimer's amyloid precursor protein
APLP1/2	Amyloid precursor-like proteins 1 and 2
APPL	β amyloid protein precursor-like
APL-1	APP-like 1
Ac	Acidic
CuBD	Cooper-binding domain
HBD	Heparin-binding domain
Aβ	Amyloid β-peptide
AD	Alzheimer's Disease
sAPPβ	Soluble APP β
AICD	Amyloid precursor protein intracellular domain
sAPPα	Soluble APP α
ER	Endoplasmic Reticulum
PM	Plasma Membrane
PTM	Posttranslationally modified
TGN	Transgolgi network
SNX	Sorting Nexins
Dab1	Disabled family member 1
ARH	Autosomal-recessive Hypercholesterolemia protein
sorLA	Sorting protein-related receptor containing LDLR class A repeats
CNS	Central Nervous System
NPC	Neural Progenitor Cell
SVZ	Subventricular Zone
SGZ	Subgranular Zone
ES	Embryonic Stem cells
NSCs	Neural Stem Cells
EGFR	Epidermal Growth Factor Receptor
DG	Dentate Gyrus
RMS	Rostral Migratory Stream
SNARE	Soluble N-ethylmaleimide sensitive factor-attachment protein receptor

FAK	Focal Adhesion Kinase
Mena	Mammalian-enabled protein
Abl	Abelson murine leukemia
Cdc42	Cell Division Cycle 42
ATP	Adenosine Triphosphate
ADP	Adenosine Diphosphate
GTP	Guanosine Triphosphate
GDP	Guanosine Diphosphate
PP	Preplate
MZ	Marginal Zone
SP	Subplate
CP	Cortical plate
GEFs	Guanine nucleotide exchange factors
GAPs	GTPase-activating proteins
PAK	P21 activated kinase
DN	Dominant Negative
WT	Wild Type
VZ	Ventricular Zone
FBS	Fetal Bovine Serum
ROI	Region of interest
DNA	Desoxyribonucleic Acid
RNA	Ribonucleic Acid
GFP	Green Fluorescent Protein
SWH	Scratch Wound Healing
F-actin	Filamentous Actin
FRAP	Fluorescent Recovery After Photobleaching
WASP	Wiskott-Aldrich syndrome protein
WAVE	WASP family verprolin-homologous protein
Arp2/3	Actin related protein 2/3
FA	Focal adhesions
KO	Knock Out
PTP1B	Tyrosine-protein phosphatise non-receptor type 1

Introduction

The Alzheimer's Amyloid Precursor Protein (APP)

Alzheimer's Amyloid Precursor Protein (APP) is ubiquitously expressed in mammalian cells and belongs to a conserved family of type 1 transmembrane glycoproteins, which is constituted also by the APP mammalian homologues amyloid precursor-like proteins APLP1 and APLP2, both showing some functional redundancy with APP, but lacking the Aβ sequence. The conservation of APP gene family extends to invertebrates, including the fruit fly *D. melanogaster* and the worm *C. elegans*, with its respective orthologues β amyloid protein precursor-like (APPL) and APP-like 1 (APL-1). All these proteins share conserved motifs within the extracellular domain and a short cytoplasmic region, which exhibits the highest sequence homology [1, 2, 3].

The human APP gene is located in chromosome 21 and contains 18 exons. The APP molecule is divided in three main domains: the large extracellular containing amino-terminal domain, the transmembrane region and the short cytoplasmic domain containing the C-terminus. The extracellular region is composed by an E2 domain, an acidic (Ac) domain, a cooper-biding domain (CuBD), and a Heparin-binding domain (HBD), all of which are conserved across species. The cytoplasmic intracellular domain presents the highest homology and contains de YENPTY motif that is conserved between homologues and is known to be required for the binding of various adaptor proteins like Fe65, Mint and Dab1 (Figure 1) [2,3].

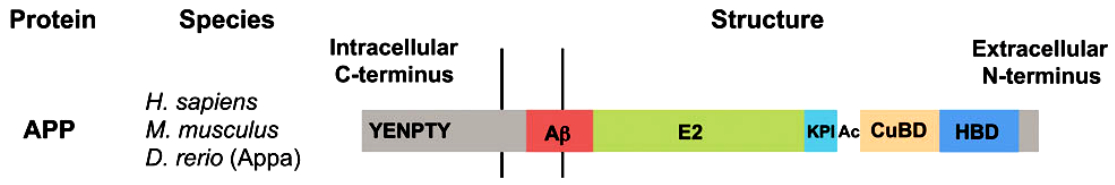

Figure 1. The domain structure of APP. The extracellular region contains an E2 domain, an acidic (Ac) domain, a copper-binding domain (CuBD) and a heparin-binding domain (HBD), all of which are conserved across species. A Kunitz protease inhibitor (KPI) domain, which is subject to alternative splicing, is also found in APP and APLP2. The intracellular domain shows the highest homology and contains the YENPTY motif that is conserved across homologs. The Aβ sequence is only present in APP. Adapted from [2]

APP is the precursor protein of Aβ, which represents the principal pathophysiologic hallmark of Alzheimer Disease (AD), being deposited in the form of amyloid plaques in AD brains. Nevertheless, the evolutionary conservation of APP and the lack of Aβ sequence in almost all APP homologues means that amyloidogenesis is unlikely to be the main function of this family of proteins [2].

Increasing evidence show that APP has physiological roles in cell adhesion, neuronal differentiation, neuronal migration, neurite outgrowth and guidance and synapse formation. Previous findings also indicate a potential role for APP as part of a complex mechanism involved in a variety of neuronal functions including normal neural development or response to traumatic brain injuries [1, 2].

APP can go through two principal processing pathways: amyloidogenic and non-amyloidogenic, depending on the secretases that cleave it. In non-pathologycal conditions, the non-amyloidogenic pathway dominates. In the amyloidogenic pathway APP is first cleaved by β-secretase producing a soluble secreted form of APP (sAPPβ) and a carboxy-terminal fragment (Bctf or C99). This is subsequently cleaved by Ɣ-secretase generating the Aβ peptide which is liberated and found in extracellular fluids such as plasma or cerebrospinal fluid, and the amyloid precursor proteins intracellular domain (AICD). In the non-amyloidogenic pathway, APP is initially cleaved by α-secretase approximately in the middle of the Aβ sequence and forms the soluble secreted sAPPα fragment and a truncated APP CTF (αCTF or C38), which lacks the amino-terminal portion of the Aβ domain. αCTF suffers Ɣ-secretase cleavage resulting in release of the Aβ peptide called P3 that seems to be pathologically irrelevant and AICD that is released into the cytosol and may have a function in nuclear signalling (Figure 2) [2,5]. Although produced in both pathways, AICD has been described as only transcriptionally functional when produced by the amyloidogenic pathway [29].

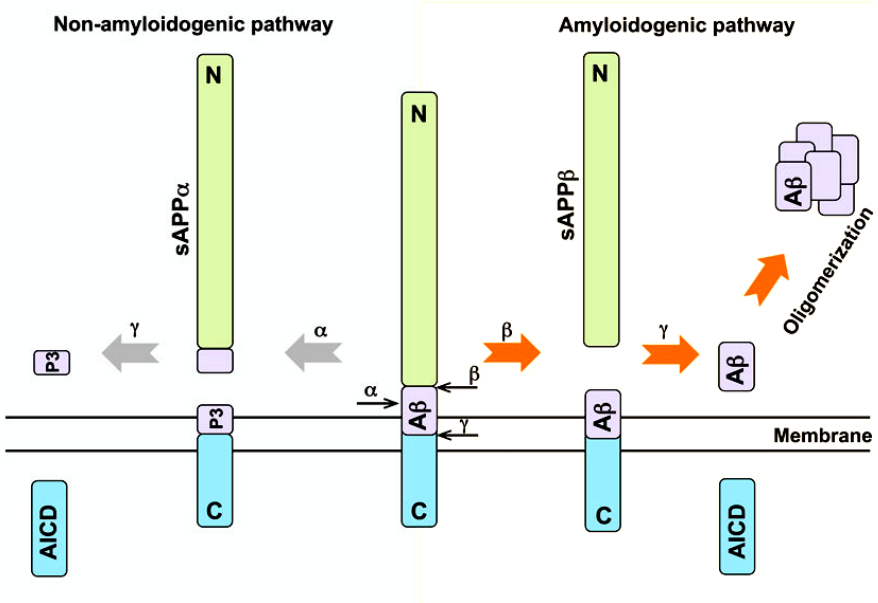

Figure 2. The proteolytic processing of APP. APP can be cleaved by α-, β- and γ-secretases; the cleavage sites of these proteases are indicated in the full-length APP shown in the center of the figure. APP can undergo amyloidogenic (right) or non-amyloidogenic (left) processing. In the amyloidogenic pathway, cleavage by β-secretase results in the formation of soluble APPβ (sAPPβ) and βAPP-CTF. The subsequent action of γ-secretase on βAPP-CTF releases Aβ from the amyloid precursor protein intracellular domain (AICD). In the nonamyloidogenic pathway, cleavage by α-secretase prevents the formation of Aβ; α-secretase cleaves within the Aβ sequence, giving rise to sAPPα and the membrane-tethered αAPP-CT, which in turn is cleaved by γ-secretase resulting in the release of the P3 peptide and AICD [2].

Amyloid Precursor Protein is produced in large quantities in the membrane of ribosomes and is metabolized very rapidly. After sorting in the Endoplasmic Reticulum (ER) via its signal peptide, while it is being transported from the ER to the Plasma Membrane (PM), APP is posttranslationally modified (PTM) by N-glycosylation in the ER and by O- glycosylation (maturation) in the Golgi, besides undergoing other PTM such as ectodomain and cytoplasmic phosphorylation and tyrosine sulphation. The majority of APP at steady state localizes to the Golgi apparatus and TGN, and from there part of the population travels by anterograde transport to the PM. In the PM, APP can be cleaved by various enzymes (secretases). APP that is not released from the cell surface is internalized within minutes of arrival at the cell surface because of the presence of its “YENPTY” internalization motif. This motif regulates the targeting of proteins to the clathrin coat vesicles and their transport, giving continuity to the endocytic pathway. These clathrin-associated vesicles mediate both steps: transport of APP from the TGN to

the cell surface or directly to an endosomal compartment. Clathrin does not bind directly to APP, instead the globular tail of each its heavy chains binds adaptor proteins which in turn bind to the cytoplasmic tail of APP containing the NPXY amino acid motif (YENPTY). Various clathrin adaptor proteins (Dab1, Fe65, ARH) bind the YENPTY motif serving as regulators of APP endocytosis.

At the cell surface APP can either be proteolyzed directly by α-secretase and then ϒ-secretase not generating Aβ, or reinternalized in clathrin-coated pits into another endosomal compartment containing ϒ-secretase and BACE1 (β-secretase), resulting in Aβ, which is then released into the extracellular space following vesicle recycling or degraded in lysossomes (Figure 3).

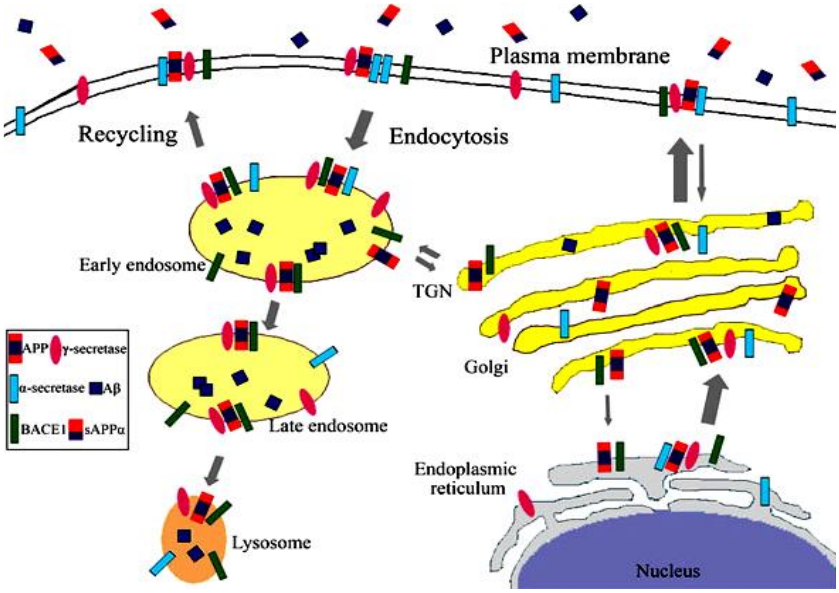

Figure 3. Typical trafficking route of APP, BACE1, α-secretase and γ-secretase. Newly synthesized APP, BACE1, α-secretase and γ-secretase traffic through the secretory pathway, from the ER to Golgi/TGN and to the plasma membrane, during which process retrieval may occur and APP may be cleaved to generate Aβ. At the plasma membrane APP is largely subjected to non-amyloidogenic processing by α-secretase to release sAPPα. Un-cleaved APP and various secretases at the plasma membrane may undergo endocytosis via early endosome to late endosome/lysosome for degradation. Acidic endosome/lysosome provides optimal environment for BACE1 activity and APP is mainly subjected to amyloidogenic processing for Aβ production in these compartments. In addition, a fraction of these proteins in endosome can be either recycled back to plasma membrane or retrieved back to TGN [7].

To complete the APP processing, retrograde communication must occur between endosomal compartments and the TGN, mediated by a complex of molecules called retromers [4, 5, 6]. VPS35 is the core of the retromer and binds the cytoplasmic tail of APP. VPS26, VPS29 and sortin nexins (SNX) 1 or 2, set up with VPS35, to form the complete functional retromer complex. Adaptor proteins such as sorLA, can bind the retromer complex to its cargo protein such as APP. The fusion between the transport vesicle and the membrane of the targeted organelle is driven by three main families of proteins: – 1) soluble N-ethylmaleimide sensitive factor-attachment protein receptor (SNARE) proteins, 2) Rab (a subfamily of the Ras superfamily of low-molecular-mass GTPases) proteins, and 3) Sec1/ Munc18 (SM) proteins. Membrane fusion and cargo delivery occur when SNAREs expressed in the membranes of the transport vesicle interact with a single SNARE protein expressed in the membrane of the recipient organelles, while the Rabs and SM proteins play important roles in mediating this interaction [6].

Protein phosphorylation is one of the mechanisms that regulate APP function, in cellular processes such as differentiation, metabolism and signal transduction [8, 9]. APP can be phosphorylated in several of its residues, two of them in the ectodomain (Ser^{198} and Ser^{206}) and eight present in the intracellular domain.

Ser655 is a phosphorylatable residue located in ^{653}YITSI^{656} motif that can be phosphorylated by PKC and CAMKII. Its phosphorylation regulates APP trafficking between Golgi, the PM, and lysosomes as well as the rate of sAPPα secretion [13, 14]. The ^{682}YENPTY^{687} domain can be modulated by phosphorylation of its tyrosine residue, Tyr682, or its upstream residue Thr668. Tyr682 is phosphorylated by different kinases such as TrkA, AbI and Src and its phosphorylation has been reported as necessary for APP interaction with the adaptor proteins ShcA and Grb2 leading to activation of MAP kinase transduction pathways [10, 11]. Cdc2, GSK3, CDK5 and other kinases phosphorylate the Thr668 residue, and this phosphorylation may impair the interaction between APP and Fe65 thus increasing APP cleavage by BACE1 and Ɣ-secretase favouring the amyloidogenic pathway. In addition, phosphorylation at Thr668 has been linked to both neurodegeneration and neurite outgrowth [12].

1. APP Neurotrophic functions

2.1. Neurogenesis

Neurogenesis is defined as the process of generating functional neurons from neural precursors [15]. It was initially believed to occur only during embryonic stages. However, forty years after the discovery of neurogenesis in the postnatal rat hippocampus, it is now established that neurogenesis continues active throughout life in discreet regions of the central nervous system (CNS) of all mammals including humans. This process occurs in most mammals in two regions: the subventricular zone (SVZ) of the lateral ventricle and in the subgranular zone (SGZ) of the dentate gyrus in the hippocampus. Outside these regions, neurogenesis is apparently extremely limited or nonexistent in the adult CNS [16].

Neurogenesis involves the generation and differentiation of stem cells into neural cells.

Stem cells are undifferentiated cells and have the ability for self-renewing division, which results in at least one daughter cell remaining as a stem cell. They also have the potential to generate multiple lineages of differentiated cell types. The properties of embryonic stem (ES) cells and adult stem cells are broadly different. ES cells are pluripotent which make them capable of differentiate into a large number of cell lineages of all three germ layer origins. Adult stem cells have much more restricted potential than ES. They are present in many adult organs and have been shown to participate in tissue repair and regeneration. Neural stem cells (NSCs), among the best studied adult stem cells, are capable of differentiating into neurons and glial cells. However, its capacity of self-renewal declines with age [17].

2.2. APP in Neurogenesis

APP, particularly through its fragments, has described roles in neurogenesis. Importantly, the type of cleavage and the amount of peptides released in APP proteolytic processing provide great complexity to the study of APP function, including in neurogenesis [28].

The soluble secreted APPα metabolite (sAPPα), a product of the non-amyloidogenic pathway, was shown to have several features related with neurogenesis. It induces neurite outgrowth, it's a proliferation factor of embryonic neural stem cells [18], regulates proliferation of neural progenitor cells (NPC) in the adult SVZ [19] and SGZ, and also regulates astrocytic fate lineage [20]. Previous studies showed that infusion of APP antisense oligonucleotides reduced proliferation of NPCs, an effect that could be reversed with infusion of sAPPα [19]. A Soluble APPα acts as well as a neuroprotectant [21], among many other effects [28, 29].

On the other hand, secreted APPβ fragment resulting from the β-secretase cleavage of APP in the amyloidogenic pathway, is considered less protective than sAPPα. APPβ has been suggested to supress neuronal differentiation and to promote astrocytic differentiation in glioma stem cells [29].

The AICD domain, by its turn, is a Fe65-dependent negative regulator of NPC proliferation [22, 29]. Evidence suggests that AICD negatively regulates the transcription of epidermal growth factor receptor (EGFR). Additionally, APP knock out mice expressing AICD showed an Aβ dependent reduction in cell proliferation and survival of NPC in the adult dentate gyrus (DG) but did not showed alterations in differentiation [23]. AICD has also been shown to induce neural apoptosis, conclusion that came from the overexpression of APP which also induces apoptosis in neurons [24].

Studies on the role of the Aβ amyloid peptide in NPC proliferation generated conflicting results. Haughey et al. 2002a showed that Aβ treatment of a human cortical NPC culture severely reduced proliferation and adversely affected differentiation of progenitor cells into neurons or astrocytes [25]. Conversely to these findings, Lopez-Toledano and Shelanski 2004 revealed that Aβ could stimulate proliferation of SVZ-derived NPCs in adult murine [26], effect that was

later discovered to be mediated by the p75 neurotrophin receptor [27]. Other studies also showed that Aβ increased embryonic stem cell proliferation [29]. Such contradictions of the Aβ role in proliferation may be due to different experimental settings, including type of Aβ peptide and concentration used.

2.3. Neuronal Migration

Cell migration is a highly organized and conserved mechanism composed of multiple steps. It takes place in normal and pathogenic processes including embryogenesis, wound healing, immune response, cancer metastasis and angiogenesis [30, 34]. In order to migrate, cells must first become polarized in response to extracellular signals. At the cell front, extension of membrane protrusions called lamellipodia form from actin assembly. At the leading edge of these structures, the cells form adhesions that make contact between the extracellular matrix (ECM) and the actin cytoskeleton. In order to move forward, the cell retracts its trailing edge by contracting actomyosin and disassembling adhesions at the rear [30]. Neuroblasts in particular, must migrate fast in order to move over long distances along the rostral migratory stream (RMS), achieving the olfactory bulb from the SVZ in only a few days [33].

To initiate migration in a developing organism, cells of the embryo go through four steps: polarization, protrusion, adhesion and retraction, also referred to as embryonic migration. As said before, in order to migrate in a certain direction, cells need to polarize in that same direction defining its front and rear. During this step cell suffers cytoplasm rearrangement and organelle repositioning, events driven by actin filaments that provide the major driving force for cell movement. The real start of movement occurs by the protrusion of the leading edge. The mechanical force for this step, called protrusive force, is given by polarization of actin filaments at the leading edge, either in the form of long, cylindrical, parallel packets called filopodia, or as a branched dendritic flat network known as lamellipodia. The addition of actin subunits in the growing-end of actin filaments pushes the membrane forward. As the membrane extends, actin filaments in the leading edge are disassembled in a process referred to as “actin treadmill”. During this processes there is addition of ATP-actin monomers to the front (barbed end) of the

actin filament, with the help of profilin and formins. Other proteins such as β-thymosin and Eps8 provide the limiting rate of polymerization. The ATP-actin subunits are hydrolysed after its incorporation in the actin-filament. ADP-actin monomers are removed from the rear (pointed end) by the action of cofilin. To complete the process, the released actin subunit substitutes its ADP with ATP so it can be incorporated in the barbed end once again (Figure 4)[34, 37].

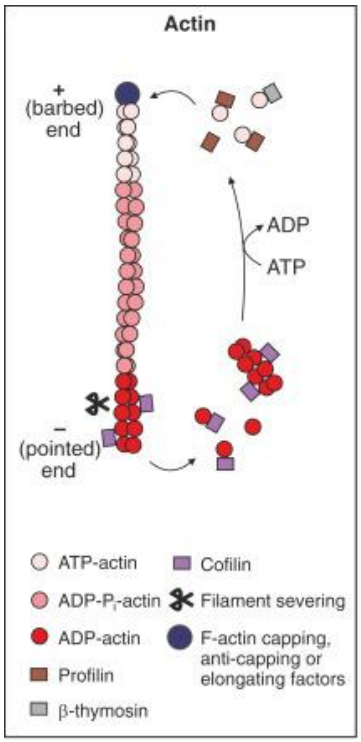

Figure 4. Schematic representation of actin treadmilling. The addition of ATP-actin monomers to the barbed end (+ end) of the actin filament is mediated through profilin and barbed-end-bound elongating factors such as formins. G-actin-sequestering proteins like β-thymosin and barbed-end capping proteins like Eps8 limit the polymerisation rate. Upon incorporation into the actin filament, hydrolysis of the ATP-actin subunits takes place. ADP-actin monomers or F-actin fragments are removed from the pointed end (– end) of the filament by the action of depolymerising or severing factors such as cofilin. Finally, to complete the cycle, the detached actin can exchange its ADP for ATP and be recruited once more to the growing filament barbed end. Adapted from [35].

At the time that the cell protrusion is formed, it needs to connect to the surrounding extracellular matrix, to stabilize and to use it as a push-off point to move forward. Through integrin clustering and recruitment of signalling and structural proteins nascent adhesions are formed that eventually maturate to focal adhesions. Integrin receptors act as the “feet” of the migrating cell by supporting adhesion to the ECM [36]. Focal adhesion formation is mediated by actin interaction with myosin II. These structures transmit the strongest forces of a migrating cell, called contractile forces. As the cell moves, focal adhesions dismantle to release the cell for a new step of migration process. At the leading edge, as focal adhesions are dismantled, new protrusions and new adhesions are formed. Focal adhesions release at the cell rear happens simultaneously to cell stretching, driven by myosin II contractility and regulated by FAK and Src signalling. This stretching force is considered to be sufficient to open stretch-activated Ca2+ channels, which activate calpain that in turn participates in focal adhesion disassemble (by the cleavage of focal adhesion proteins such as talin, vinculin and FAK). The release of adhesions at the trailing edge allows the preservation of cell polarity at the front and promotes its activity creating a positive feedback that contributes to the continuity of the migration cycle (Figure 5) [34, 37].

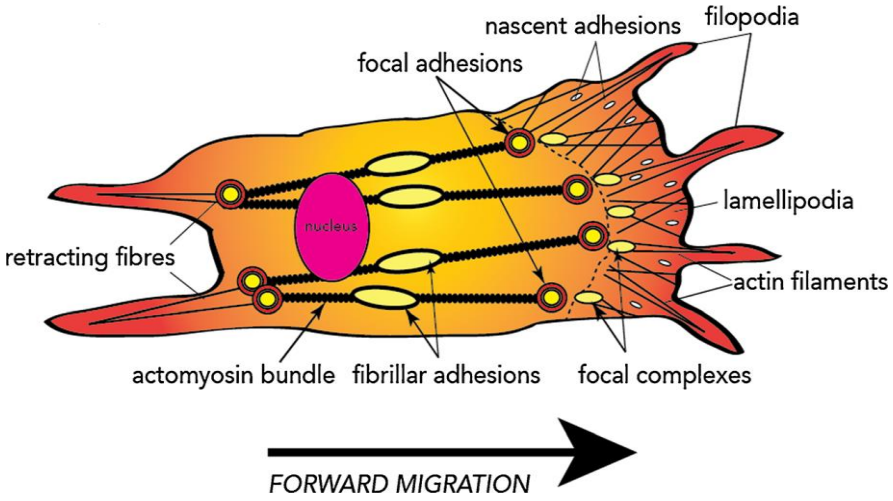

Figure 5. Overview of the structures involved in cell adhesion and migration. Lamellipodia and filopodia form from actin and are used during adhesion and migration. Nascent adhesions maturate to focal adhesions and connect the cell to the extracellular matrix. As the cell moves forward, focal adhesions are dismantled and new adhesions and new protrusions are formed at the leading edge [53].

Cells in culture generally exhibit spontaneous, stimuli-independent polarization and migration, while in the developing embryo cell migration is accurately coordinated by extracellular signals that define the timing, direction and the final destination of the migrating cells. Such signals control the complex events that occur during embryogenesis, including gastrulation, patterning, and tissue and organ formation. Disturbance of these signals lead to severe abnormalities of embryogenesis [34].

The migration of neurons in the developing neocortex results in the formation of an orderly 6-layered structure, described as inside-out migration. The first neurons to leave the proliferative zone initially form a primitive structure called preplate (PP). Once the PP is complete, the next group of migrating neurons splits the preplate into two separate regions, the marginal zone (MZ) and the subplate (SP). These neurons start to form a new region between the MZ and SP that is the emerging cortical plate (CP). The first neurons to arrive in the CP are the cells that will form progressively more superficial layers of cortex [50].

In the adult brain, neuroblasts are continuously generated in the SVZ. These neuroblasts migrate rapidly in the RMS, forward to the olfactory bulb where they maturate and are integrated in the neural circuitry. Neuroblasts migrate through mechanisms that are unique to the adult brain and are not involved in developing brain migration [31].

Neuronal migration in the adult brain happens in a saltatory manner that involves leading-process extension, swelling formation and centrosomal migration, and somal translocation (Figure 6). In the first step (leading-process extension), filamentous (F)-actin accumulates at the end of the leading process during extension (phenomena regulated by the Rho family of small GTPases and downstream F-actin modulators). Extension of the leading process is also carried out by microtubules [31]. In the second step (swelling formation and centrosomal migration) the term swelling refers to a dilation in the cytosol that forms in the proximal part of the leading edge. These dilations are novel structures that are not apparent in other cell types. Their location predicts where the nucleus will be moved to in the end of the saltatory movement [31]. The swelling contains intracellular organelles such as the centrosome that organizes microtubules and

controls microtubules networks, Golgi apparatus and mitochondria. The third and last step (somal translocation) is controlled by actomyosin contractions under the regulation of RhoA signaling. During this last step, F-actin accumulation and Myosin II activity are observed at the proximal part of the leading edge and at the rear of the cell [32]. These migration behaviours are influenced by extracellular hints such as ions, guidance molecules and trophic factors [33].

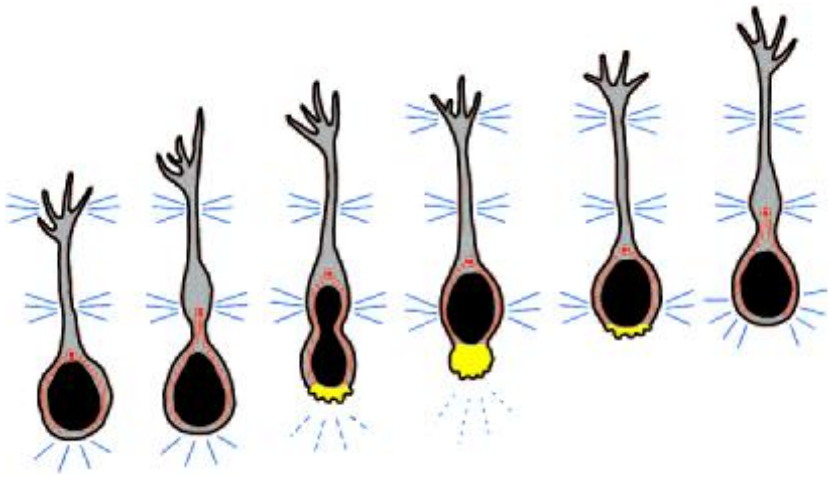

Figure 6. A model for cytoskeletal coordination during cycles of saltatory neuronal migration. As the leading process extends, it makes adhesive contacts with the extracellular matrix (blue). After the growth of the leading process past this position, a cytoplasmic dilation forms distal to the cell nucleus. Before the onset of nuclear movement, the centrosome (red dot) is moved by an as-yet unknown mechanism into the forming dilation. Microtubules (red lines) within the cell soma form longitudinal arrays (possibly as a result of pulling forces generated by centrosome movement) and vacate the cell rear. The nucleus then translocates toward the centrosome along the longitudinal microtubule arrays. We postulate that an absence of microtubules at the cell rear triggers contractions mediated by myosin II (yellow), which generates a pushing force on the nucleus and serves to break adhesions at the cell rear. Nuclear movement stops as the nucleus enters the former location of the dilation, and the process begins again [31].

2.4. APP in cell migration

APP silencing leads to defects in neuronal migration. A study using *in utero* electroporation of shRNA showed that neuronal precursor cells in embryonic cortex require APP to efficiently migrate to the nascent cortical plate [52, 11].

APP is generally accepted as a contributing protein to cell adhesion via its extracellular domain. The E1 and E2 regions of APP interact with extracellular matrix proteins. These regions can also interact with themselves forming homo (with APP) or heterodimers (with APLP's). APP/APLP's are also suggested as synaptic adhesion molecules [52].

The extracellular sequence of APP interacts with various extracellular matrix components, such as heparin, collagen type I and laminin. Cytoplasmic domains of APP also facilitate cell-cell adhesion through transcellular interactions [51].

Evidence suggests that APP_{695} (the most predominant form of APP in the brain) itself can regulate multiple aspects of neuronal motility including migration. Additionally, the role of APP in neuronal migration is also related with dozens of binding partners and cytoplasmic proteins such as Fe65, a brain-enriched, developmentally regulated adaptor protein that was identified as a partner of APP.

Coexpression of APP and Fe65 greatly increased the effect of APP on cell movement. Fe65 interacts with the YENPTY motif of APP and its overexpression is associated with an enhanced APP translocation to cell surface and proteolytic processing. Transfection with both APP and Fe65 accelerated wound closure in wound healing assays performed on MDCK (Madin Darby Canine Kidney) cells. The effect of either protein is enhanced by the presence of the other. It has also been shown that together these proteins are involved in lamellipodia motility as part of a larger macromolecular complex. Sabo et al. 2001 proposed that some of the effects of this macromolecular complex are mediated by Mena [38, 39]. Mena is an Abl-associated signalling protein involved in actin dynamics regulation in lamellipodia. APP and Fe65 colocalize with Mena and actin and specifically concentrate with β1-integrin in focal complexes (dynamic adhesion sites) but not in focal adhesions that are more static structures.

Nevertheless, besides these, very little is known about the underlying cellular and molecular mechanisms of APP influence on cell migration.

2.5. Cdc42 in cell migration

Cdc42 is a member of the Rho family of small GTPases expressed in many cell types including neurons [45]. It is active when bound to GTP and inactive when bound to GDP. Its activation occurs with the help of guanine nucleotide exchange factors (GEFs) that exchange GDP for GTP, and its inactivation is mediated by GTPase-activating proteins (GAPs), which promotes the hydrolysis of GTP to GDP. Cdc42 is one of the most conserved members of the Rho family across eukaryotic species, together with Rac and Rho. It is present in plants, fungi and

animals. The roles of these proteins in cell migration have already been established years ago [40]. Besides their participation in cell migration, Rho GTPases are also involved in signal transduction pathways that link receptors in cell surface to a variety of intracellular responses. This family of monomeric G proteins regulate actin cytoskeleton, control cell polarity, gene expression, microtubule dynamics and vesicular trafficking [49].

Cdc42 is one of the major regulators of cell polarity establishment, but its activity has also been associated with proliferation, neurite outgrowth and early dendritic growth, cell division, shape, motility, polarity and spine maturation of adult hippocampal NPCs [45, 46, 47].

In a study performed in HeLa cells transfected with both Cdc42 WT (wild type) and Cdc42 DN (dominant negative – a mutant form of Cdc42 with a threonine to asparagine substitution at residue 17 that abolishes the protein's affinity for GTP and reduces its affinity for GDP, so Cdc42 DN is always in wither a nucleotide free state or in its inactive GDP-bound state) – cells transfected with Cdc42 WT showed more filopodia that the Cdc42 DN (around the double). A migration assay using transwells was also performed, and the migrating capacity of cells transfected with Cdc42 WT was significantly higher than those transfected with Cdc42 DN [44].

When active, Cdc42 activates its downstream targets of the WASP/WAVE family such as WAVE2, which in turn activate the Arp2/3 complex that regulates the formation of branches on actin filaments at the leading edge. Additionally to Rho and Rac, Cdc42 is present in lamellipodia and contributes to lamellipodium extension and formation acting essentially through formins. In mouse endothelial cells lacking WAVE2, lamellipodium formation is extremely disrupted and migration is reduced, which proves the role of WAVE2 [34, 42].

Moreover, the family of Rac/Cdc42-activated PAK (P21 activated kinases) participates in integrin-based adhesion turnover [43].

Besides that, Cdc42 plays an important role in migratory persistence, acting through the PAR complex [34, 40, 41]. Other studies also refer that Cdc42 act in the front of the cell controlling the direction of migration in response to extracellular cues and, in epithelial cells, Cdc42 as well as Rac are also involved in the

assembly of adherens junctions, also through the PAR complex [47]. Junctions are posteriorly stabilized via association of actin filaments, also with participation of Rho GTPases [46].

Figure 7 summarizes the functions of Rho GTPases in cell migration.

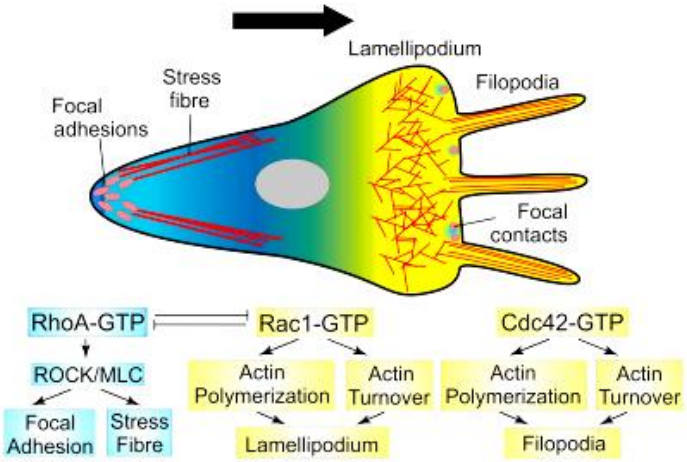

Figure 7. Rho GTPases and cell protrusion control. The typical Rho GTPases – RhoA, Rac1 and Cdc42 – play a crucial role in controlling cell polarity. These three Rho GTPases regulate different aspects of cytoskeleton dynamics. Cdc42 has been shown to be involved in controlling the actin cytoskeleton present in protrusions known as filopodia. Rac1 promotes the formation of lamellipodia – large, flattened and ruffling protrusions – by regulating actin polymerization. The three Rho isoforms – RhoA, RhoB and RhoC – can induce stress fibre formation [64].

In a previous study from our lab [65], which started to characterize the role of APP in neuronal-like cell migration, APP appeared to have a role in the persistence of direction in cell migration. This idea was here revisited for final confirmation, and one of the potential underlying mechanisms, via Cdc42 activation, explored, since we have also observed that APP binds to an activates Cdc42 in HeLa cells (unpublished data [65]).

Aims of the work

In this project we aimed to characterize the role of APP in cell migration, particularly in neuronal-like cells, and its interdependency with Cdc42 in various underlying processes. For that, the following principal goals were established:

- To confirm the influence of APP in directional persistent migration in neuronal-like cells, and its interdependence of Cdc42;

- To analyse the influence of APP in velocity of migration and distance migrated by neuronal-like cells, and its interdependence of Cdc42;

- To study the role of APP and Cdc42 in the acquisition of a migratory phenotype;

- To study the effects of APP in F-actin dynamics in migrating neuronal-like cells.

Materials and Methods

Amplification and Purification of cDNAs

The cDNAs used in this thesis – GFP (eGFP-N1, Clontech), APP-GFP (produced in [13]), DsRed-Cdc42 WT and DN (dominant negative) (Addgene; fused to DsRed as in [68] - were first amplified for stock maintenance, and purified.

1.1. Competent Cells

To prepare competent cells, we started with a pre-inoculum in the day before, where we inoculated one colony of JM-109 and BL21 (DE3) bacteria in separate tubes with 10 mL of SOB each, and incubate them overnight at 37ºC with 180 rpm agitation.

In the following day, 1 mL of each pre-inoculum was transferred to Erlenmeyers containing 50 mL of SOB and further incubated at 37ºC, 180 rpm agitation for 1-3h. 3h hours later, 1 mL of each culture was pipetted into a cuvette to measure optical density at 550 nm. SOB medium was used as negative control. Optical density should range between 0.3-0.5. Once this value was achieved, Erlenmeyers were placed on ice for 15 minutes. Then, the content of each Erlenmeyer was transferred to a 50 mL Falcon conic tube, and centrifuged at 4000 rpm, 4ºC for 5 minutes. Falcons were placed on ice and supernatant was discarded. 15 mL of solution I was added and the pellet ressuspended. Falcons were placed on ice for 15 minutes, and once again centrifuged with the same conditions. The pellet was ressuspended in 3 mL of solution II and divided in aliquots of 100 µL in Eppenforfs that were frozen in liquid nitrogen and then stored at -80ºC. Composition of solutions I and II, as of others, are described in Appendix.

1.2. Bacterial transformation

JM-109 competent cells were thawed on ice and 1 µL of each cDNA to amplify were added to 100 µL aliquots of competent cells. Cells were incubated on ice for 30 minutes, posteriorly subjected to heat shock by incubation in a 42ºC bath for 45 seconds, and then rapidly transferred to ice for 2 minutes. 900 µL of LB medium was added to the cells, followed by incubation at 37ºC for 60 minutes. Cells were finally centrifuged at 14.000 rpm for 1 minute, the supernatant discarded, and the

pellet ressuspended in the remaining volume to be plated in LB/kanamicyn agar plates (see Appendix). Plates were incubated at 37ºC over night.

1.3. DNA purification by “Miniprep”

In the day before, one colony of each transformed cell (prepared in 1.2 was inoculated in 4.5 mL of LB medium containing 4.5 µL of kanamicyn and incubated overnight at 37ºC and a 180 rpm agitation. In the next morning, 1.5 mL of each inoculum was transferred to a microtube and centrifuged at 14.000 rpm for 30 seconds. The supernatant was discarded and these two steps repeated three times. Subsequently, 100 µL of cold solution I were added and the microtubes vortexed vigorously. After that, 200 µL of solution II were added, microtubes mixed by inversion 5 times, and placed on ice for 2 minutes. Posteriorly, 150 µL of solution III were added, microtubes were inverted a few times and placed on ice for 5 minutes. The suspension was centrifuged at 14,000 rpm for 7 minutes and the supernatants transferred to new microtubes. In order to precipitate the nucleic acids present in the supernatant, the ethanol precipitation protocol was performed starting with 2 volumes of 100 % ethanol. Tubes were vortexed and placed on ice for 2 minutes. Then cells were centrifuged at 14,000 rpm for 10 minutes. Supernatant was discarded, and 1 mL of 70% ethanol was added. Microubes were mixed by inversion a couple of times, placed on ice for 2 minutes and again inverted to ensure the quality of the DNA. Tubes were further centrifuged at 14,000 rpm for 2 minutes, the supernatant was discarded, and pellets were left to dry. Once dried, 50 µL of RNAse-containing water was added to each tube, DNA left to dissolve, and its concentration and purity measured with a DS-11 Spectrophotometer (DeNovix). DNA was stored at -20ºC. Composition of solutions I, II and III are described in Appendix.

2. SH-SY5Y cell line – culture and maintenance

SH-SY5Y (ATCC CRL-2266) is a twice subcloned cell line derived from the SH-SY subclone of the parental SK-N-SH cell line, isolated from a human neuroblastoma. It is a model for neuronal differentiation, since the cells can be converted to functional neuronal-like cells [66]. SH-SY5Y cells were maintained in Minimal Essential Medium (MEM):F12 (1:1) (Gibco) containing 10% fetal bovine serum (FBS), 2 mM L-glutamine and 1% antibiotic/antimycotic mix (Gibco) in a 5% CO_2 humidified incubator at 37ºC.

SH-SY5Y cells were maintained by changing the medium two to three times per week, and cells were passed when cell confluence achieved approximately 90%. To do so, 1 mL of trypsin was added to a 100 mm plate for about 3 minutes in the humidified incubator to detach cells. Cells were ressupended in 5 mL of medium. This suspension was centrifuged at 1.000 rpm for 3 minutes, and the supernatant was discarded. The pellet of cells was ressuspended in 10 mL of fresh medium. If cells were only to be maintained, usually 1 mL of this new cell suspension was plated in 100 mm plates with 9 mL of fresh medium. If we were about to start an experiment, cells were scored in a Neubauer Chamber (Celoromics), using the vital dye Trypan blue, to plate an exact quantity. Cells were stored in MEM:F12 with 10% FBS and 5-20% DMSO and freezed in liquid nitrogen in 1mL cryopreservation vials. When needed, vials were thawed and the cells' aliquot ressuspended in medium and maintained as described above.

3. Transient transfection of SH-SY5Y cells by Turbofect™ reagent

In order to study the roles of APP and Cdc42 in cell migration, GFP and Wt APP-GFP cDNA's were used in single transfections, and both Wt APP-GFP and DsRed-Cdc42 Wt or DN were used for co-transfections. For the analysis of the cytoskeleton dynamics, the LifeAct-RFP cDNA (Ibidi), which is a red fluorescent marker of filamentous actin (F-actin), was used in co-transfections with GFP or APP-GFP cDNAs.

Transfections were performed using Turbofect™ from Thermo Scientific. Turbofect is a cationic polymer that forms compact, stable, positively charged complexes with DNA, protecting it from degradation and facilitating gene delivery into eukaryotic cells. Turbofect demonstrates superior transfection efficiency and minimal toxicity when compared to lipid-based or other polymer-based transfection reagents. Cells were plated in 35 mm or six-well plates until reaching ~ 85% confluency. 2 µg of each DNA were diluted in 100 µL of serum-free growth medium. After briefly vortexed, 4 µL of Turbofect were added to each 2 µg of diluted DNA(s). The mixture was vortexed and incubated at room temperature for 15-20 minutes. During this period, cell medium was replaced by fresh medium in the 35 mm plates. The mixture was subsequently added drop by drop to each plate, with gentle agitation to achieve even distribution. Cells were incubated at 37ºC in a CO_2 incubator. After 6h medium was replaced and cells incubated for further 17-20h.

4. Scratch Wound Healing (SWH) Assays

To give continuity to the previous work on cell migration performed by CSilva in our lab [65], SWH assays were performed as before, due to its simple application and low-cost.

750,000 SH-SY5Y cells were plated on six well plates or single 35 mm plates and transfected with the cDNAs as above described. Plates were precisely marked on the bottom with two parallel horizontal, and two parallel vertical lines with a permanent pen, to serve as guidance axes. Following, a wound was created by gently scratching the cell monolayer, between each two parallel lines, with a sterile P10 pipette tip. After performing the wound, cells were washed with PBS and the medium replaced by complete fresh medium immediately.

Plates were maintained in 37ºC/5%CO_2 and cells' migration was monitored hourly during 13h Fluorescent and phase contrast (PhC) images of each wound were taken immediately after the scratch (t0) in selected cell-free wound areas of each plate, for all conditions. These images were obtained using an automated screening microscope (In Cell Analyzer) with a 10x objective.

The Migratory path of SH-SY5Y cells was analyzed using the acquired images and the MTrackJ plug-in of the ImageJ software (NIH). 30 cells were chosen for each condition, and their trajectory followed over the time.

5. Immunocitochemistry for assessing a migratory phenotype

In order to analyze the migratory phenotype of transfected cells, 750,000 SH-SY5Y adherent cells were plated onto glass coverslips inside six well plates, and transfected with the above described cDNAs. After 17h of incubation, cells were fixed with a 4% paraformaldehyde/PBS solution for 30 minutes and permeabilized with a 0.2% Triton in PBS solution for 10 minutes. As actin is a cytoskeleton protein involved in the acquisition of a migratory morphology, F-actin was labeled by incubating cells for 1h with Alexa Fluor® 568 Phalloidin (Life Technologies) diluted 1:50 in PBS with 1% BSA. Cells were further washed 3 times with PBS-T (0.05%) Tween and 1 last time with PBS. Cells were finally mounted on glass slides with antifading reagent, that contained or not DAPI (Vectashield, Vector Laboratories).

Epifluorescence microscopy analysis of migrating cells was carried out using an Olympus IX-81 microscope equipped with a LC Plan FI 20X/0.40 and a Plan Apo 100x/1.4 objectives.

6. Fluorescence Recovery after Photobleaching (FRAP)

Fluorescence Recovery after Photobleaching is a widely used technique that allows characterization of the mobility of cell's molecules. It requires a microscope, a light source able to deliver high potency light, and a fluorescent probe coupled to the molecule of interest. Images using a low light level are acquired to determine the initial fluorescence, and then high laser potency is applied to the regions of interest (ROIs) for a short time, to bleach the fluorescent probe. In case the molecules are not mobile, the bleached area will remain black. If the fluorescing molecules can move, either by diffusion or by active processes, the bleached area will recover fluorescence again. Following bleaching, the bleached ROI is further

imaged with a low light level (to prevent further bleaching) to monitor the redistribution of molecules via recovery of fluorescence [59, 60]. Figure 8 represents a standard FRAP curve.

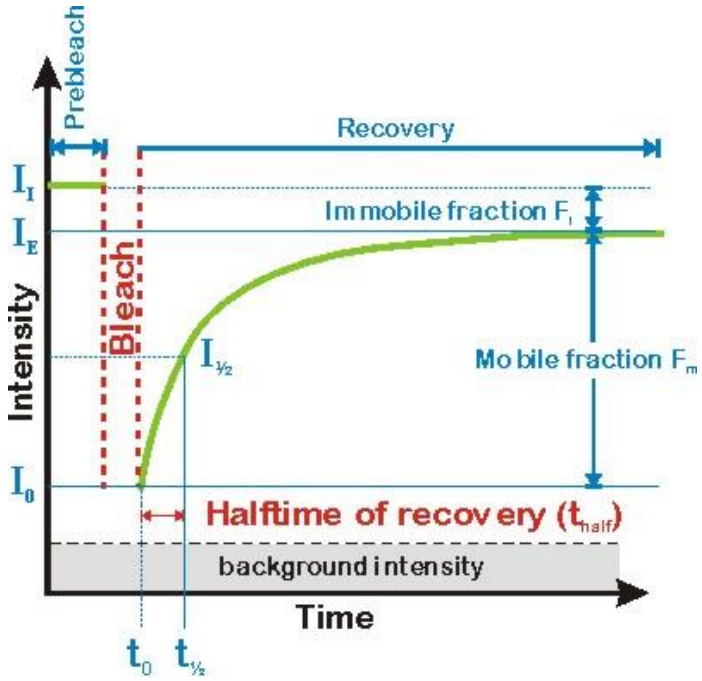

Figure 8. Schematic represention of a standart FRAP recovery curve. Fluorescence intensities of a bleached ROI in a time series. I_I: Initial Intensity; I_E: Endvalue of the recovered intensity; $I_{1/2}$: half recovered intensity corresponding to $t_{1/2}$; I_0: Intensity at timepoint t_0; t_{half}: halftime of recovery [62].

We performed a FRAP assay to monitor the effect of APP overexpression on the F-actin cytoskeleton's dynamics in migrating cells. SH-SY5Y cells co-expressing LifeAct-RFP and GFP or APP-GFP, were subjected to a SWH assay for about 4h, and medium was replaced for phenol-red free MEM, to reduce nonspecific background intensity and improve the signal-to-noise ratio upon imaging. FRAP assays were conducted on a Leica SP5 laser scanning inverted microscope equipped with a Plan-Apochromat 63x/1.4 oil objective and an enclosed thermostatted stage that kept cells alive at 37ºC and 5% CO2. Two ROIs were selected for each cell: the cell front and rear. Magnification, laser power and detector gains were similar across samples. The F-actin red fluorescence was photobleached using 561 nm laser line at full power, with a pixel dwell time of

about 30 seconds. Images were taken until the recovered fluorescence intensity of the ROIs reached a plateau.
LAS AF Lite software version 2.6.0.7266 was used for image acquisition and analysis. Fluorescence recoveries in the bleached regions during the time series were quantified.

7. Statistical Analysis

Data is expressed as mean ± SEM (standard error of the mean) from 2-4 independent assays. In SWH, FRAP and ICC assays, the number of cells analysed are indicated. Statistical significance analysis was conducted by two-tailed student t-test using the GraphPad Prism software. Differences considered statistically significant are indicated in the respective legends.

Results

1. Directional Persistence

1.1. Optimization of the Scratch Wound Healing Assay

Before start using the SWH assay, some conditions needed to be optimized, such as the amount of DNA to transfect, cell confluence, the time intervals between microphotographs and also the total time of the assay.

For DNA transfection, 1.5 µg and 2 µg of cDNA were tested. 1.5 µg was enough for a reasonable GFP expression but not so much for the bigger APP-GFP cDNA, harder to transfect. So, we decided to use 2 µg for all cDNAs, an amount that was also ok for the DsRed-Cdc42 cDNAs expression. Cell confluence was also an important aspect to consider once we observed that transfection caused the death of some cells. Since a confluence between 70-90% is the ideal to successfully transfect cells, but to perform the wound there must not be much space between cells, an initial confluence around 85% was used.

We knew from previous work in our lab [65] that at 24h SH-SY5Y cells presented a reasonable state of wound closure (60-80%). However, as we here aimed to confirm the role of APP in directional persistent migration, and to study the influence of Cdc42 in that process, we monitored cells in an earlier period of migration. The SWH assays were initially performed for 8h and microphotographs taken manually with intervals of 2h, which were too spaced for individual cell monitoring. In order to maintain cells in optimal conditions, we decided to use an automated screening microscope (In Cell Analyzer) where cells were maintained in an incubator at 37ºC and 5% CO2, and microphotographs automatically taken with intervals of 1h, for a longer period of time (13h). These allowed cells to migrate more into the wound, and to increase the number of individual transfected cells that we were able to track.

1.2. APP and Cdc42 in Directional Persistent Migration

We previously observed in our lab that APP-transfected SH-SY5Y neuroblastoma cells appear to have a more directed pattern of migration than GFP-expressing control cells [65].

To confirm that APP actually influences the cells' directional persistence in migration, and analyse if this effect occurs through activation of the Cdc42 pathway, SH-SY5Y cells were transfected with the GFP vector (control) or the APP-GFP cDNAs, or co-transfected with APP-GFP and DsRed-Cdc42 (Wt or DN). A SWH assay was performed, and cells left to migrate and monitored in an automated screening microscope; microphotographs were taken hourly for 13 hours.

Figure 9 represents the wound area for the GFP (A) and APP-GFP (B) conditions. We can see that 13 hours after the wound was made some cells migrated to the wound area and other are closer to the edge of the wound.

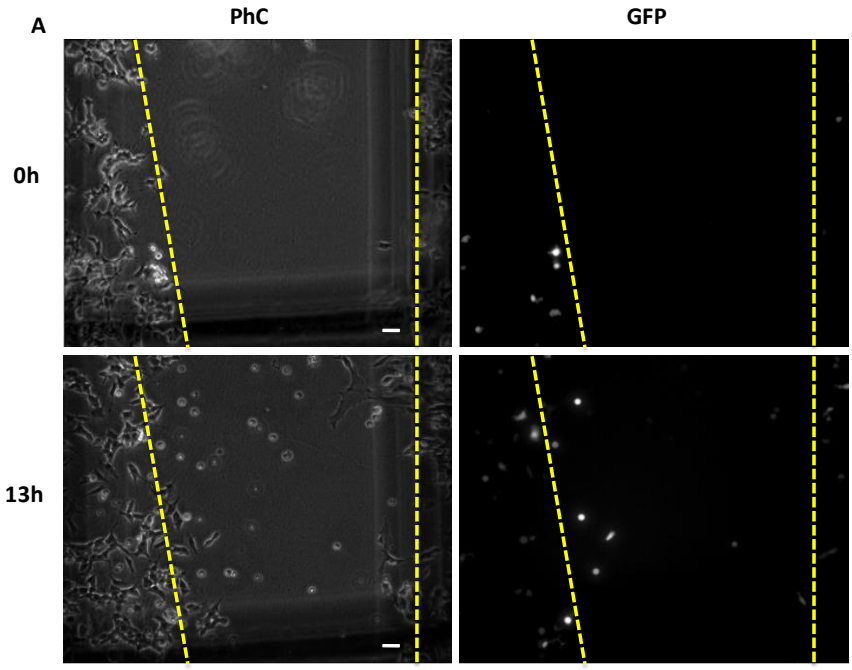

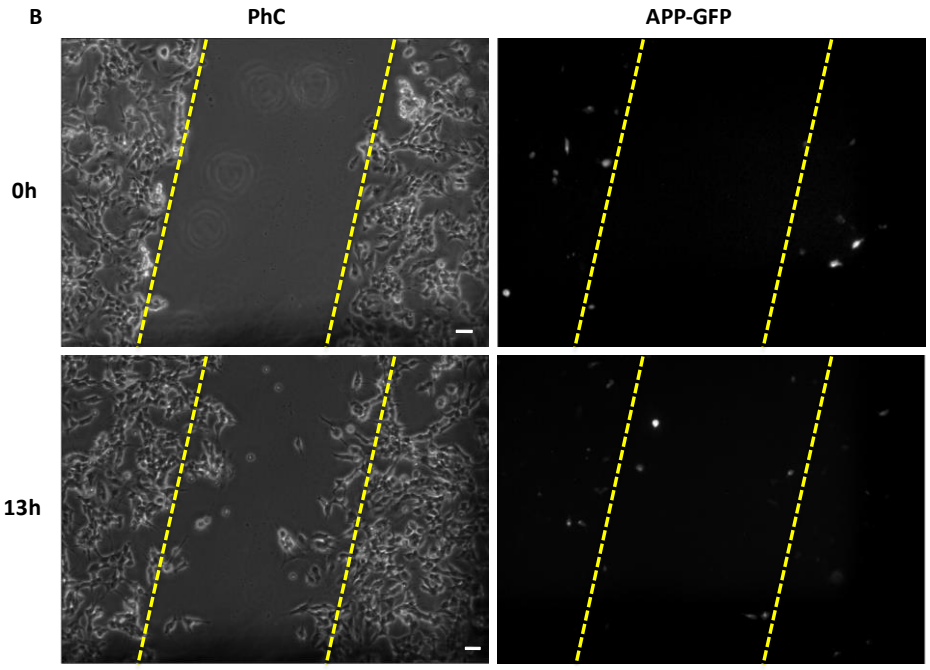

Figure 9. Microphotographs of the wound area at 0h and 13h of GFP condition (control cells) and APP-GFP transfected cells. A. Microphotographs of the wound area of GFP transfected SH-SY5Y cells at 0h and 13h of a SWH assay. **B.** Microphotographs of the wound area of APP-GFP transfected cells at 0h and 13h of a SWH assay. Scale bar - 10 µm.

As a first analysis of these SWH assays, we determined the cellular enrichment inside the wound for the different conditions. To evaluate the gain of transfected cells in the wound, a quantitative analysis of the cellular recruitment was performed. Total number of cells in PhC (control) images and green fluorescing cells (GFP or APP-GFP transfected), were scored at time 0 outside the wound, and at 13h inside the wound, to analyse if there was an enrichment in transfected cells in the population inside the wound area.

Results were calculated as fold increase over each 'outside of the wound' transfection levels, and are depicted in Figure 10.

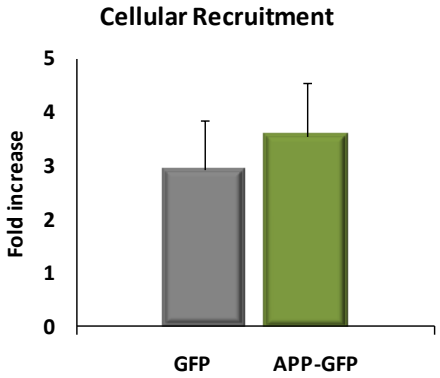

Figure 10. Increased recruitment of GFP and APP-GFP transfected cells to the wound area. Representative graphs of the quantitative analysis of the gain of transfected cells in the wound area at 13h of a SWH assay.

This analysis allows us to verify that the percentage of transfected cells in the population increased in the wound, when compared with the outside regions. Also, there was a slightly higher recruitment of APP-GFP expressing cells (3.6 ± 1.0 times higher in the wound area than outside), relatively to GFP transfected cells (2.9 ± 0.9), although not significant.

In order to evaluate the cells' migration pattern and to calculate their migration velocity and distance, it was necessary to track the green fluorescing cells. Figure 11 represents the tracking method used. We can follow the movements of the cells over time and define their trajectory. Cells were tracked with Fiji (Image J) software, using the MTrackJ plug-in.

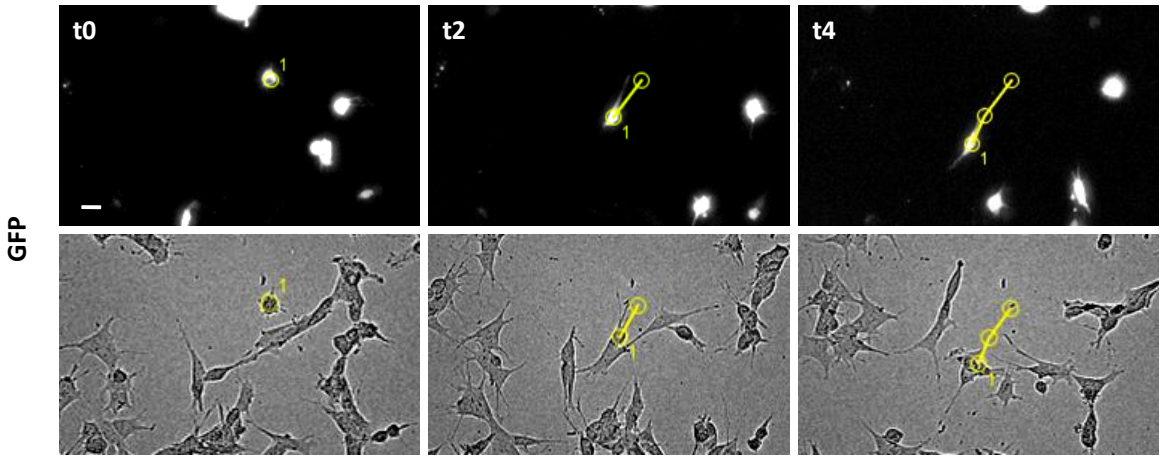

Figure 11. **Microphotographs of cells migrating over time.** Representative microphotographs of a GFP expressing SH-SY5Y cell's trajectory over time (0, 2 and 4 hours). Yellow circles represent the last position of the cell and yellow bars represent the trajectory of the cell. Scale bar -10 µm.

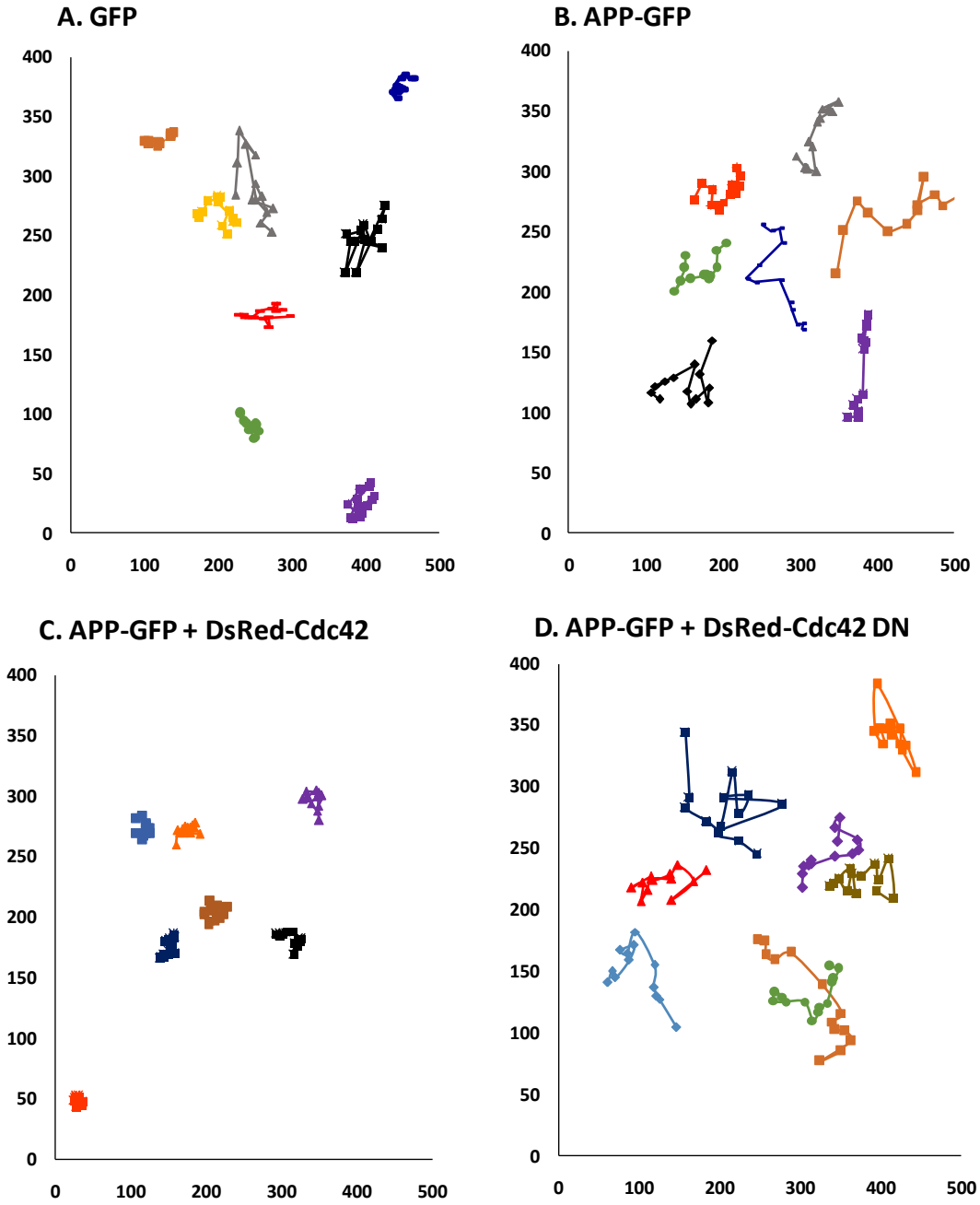

Figure 12. Representative graphs of SH-SY5Y trajectory in a 13h SWH assay, based on hourly coordinates. Representative cells of a population of A. GFP transfected cells (N=2). **B.** APP-GFP transfected cells (N=2). **C.** APP-GFP and DsRed-Cdc42 co-transfected cells (N=4). **D.** APP-GFP and DsRed-Cdc42 DN co-transfected cells (N=4). 30 cells per condition.

In the microphotographs of the SWH assays, random cells that entered the wound were chosen and tracked each hour of the 13h. The X/Y coordinates at each hour were extracted for each cell. Thirty cells per condition of at least two biological independent assays were tracked. Several cells' trajectories were graphically represented over time to visually evaluate the persistence in the migration's direction (Figure 12).

Figure 12 allows us to perform a qualitative analysis of the cells' direction and trajectory. The majority of GFP-transfected control cells (Figure 12A) migrated randomly in a restricted area, less directed to an end point than APP transfected cells (Figure 12B) that, contrarily to GFP expressing cells, showed a more constant direction in their migration. When co-transfected with APP-GFP, DsRed-Cdc42 Wt was prejudicial to cells persistence in direction (Figure 12C), returning to a migration profile more similar to GFP transfected cells. Co-transfection of APP-GFP with Dsred-Cdc42 DN (Figure 12D) increased the directed trajectory over GFP control cells and returned to more direct migrated trajectories as the ones observed for solely APP-GFP transfected cells.

A quantitative analysis was performed to confirm the apparent differences in the persistence of direction of migration. To measure the directionality of migration, a method called "out-of-track" percentage was used [65]. For that, the linear distance between the end and initial points of migration was calculated as well as the totally migrated distance over time (sum of hourly migrated distances). The numerical difference between these, presented as percentage of the linear migration, reflects deviations of the linear track, a value inversely proportional to the migration efficiency. Results of this analysis are graphically represented in figure 13.

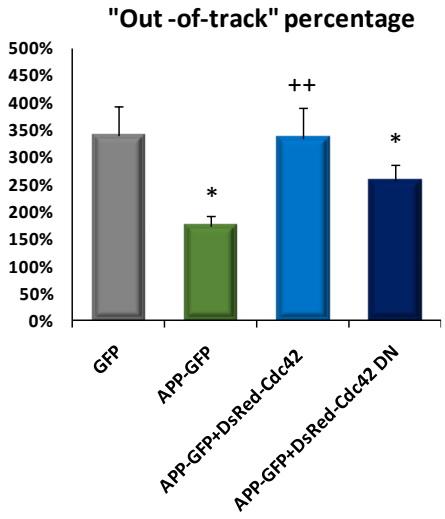

Figure 13. "**Out-of-track" percentages of migratory SH-SY5Y transfected cells in a SWH assay.** Representative graph of "out-of-track" percentages of SH-SY5Y cells transfected with GFP (control), APP-GFP, or co-transfected with APP-GFP and DsRed-Cdc42 Wt or DN, in a scratch wound healing assay. Data was calculated from single cell tracks as in figure 12. Statistically significant differences, determined by the two-tailed unpaired t-test: *p<0.05, ++p<0.01, for data against GFP control conditions (*), and for comparisons between co-transfected conditions and solely APP-GFP transfection (+).

In figure 13 it is possible to confirm that APP-GFP expressing cells have a more directed pattern of migration, with a lower percentage of "out-of-track" (173.9 ± 18.3%) than control cells (338.3 ± 54.9%). The overexpression of Cdc42 Wt in APP-GFP transfected cells significantly increases the deviation of these cells from the direct track, when compared to the solely APP-GFP expressing cells, with an "out-of-track" percentage very similar to control cells (334.0 ± 55.9%). When Cdc42 was overexpressed but its catalytic activity inhibited (by co-transfection with Cdc42 DN), the cells' deviation to the final direct track reduces to 255.7 ± 30.9%, which is not as low as APP-GFP single transfected cells, although the difference was not considered statistically significant.

Migration efficiency is also based on the distance and velocity of migrating cells. In this analysis we calculated the average total distance migrated by the cells during the 13 hours of the assay based on hourly coordinates, and its average velocity of migration. Results are depicted in Figure 14.

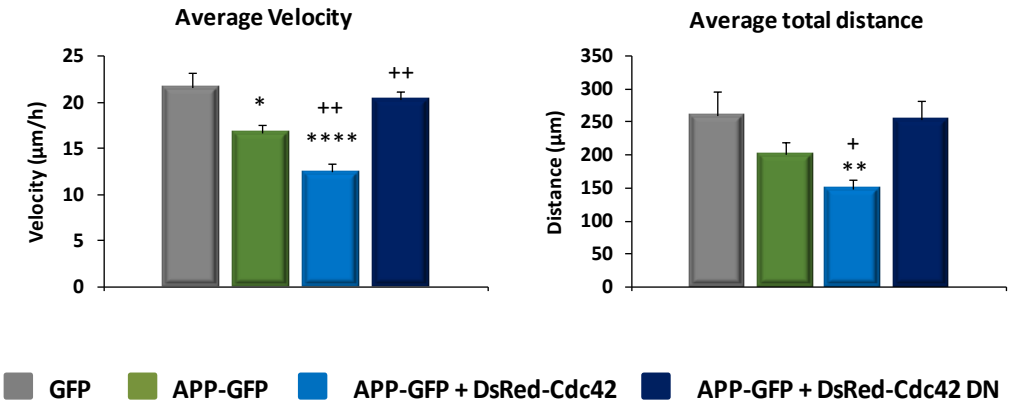

Figure 14. Average velocity and average total distance migrated by SH-SY5Y transfected cells in a SWH assay. Representative graphs of average velocity and average total distance migrated by SH-SY5Y cells transfected with GFP (control), APP-GFP, or co-transfected with APP-GFP and DsRed-Cdc42 Wt or DN, in a scratch wound healing assay. The analysis was based on cells' X/Y coordinates, collected hourly for 13h, using the ImageJ software. Statistically significant differences, determined by the two-tailed unpaired t-test: */+p<0.05, **/++p<0.01, ****p<0.0001 for data against GFP control conditions (*), and for comparisons between co-transfected conditions and solely APP-GFP transfection (+).

It was possible to verify that APP overexpression decreases both the total distance (from 260.3 ± 36.9 to 200.6 ± 19.8 µm) and the velocity of the cells (from 21.7 ± 1.6 to 16.7 ± 0.8 µm/h), comparing with GFP control levels. When Cdc42 Wt was co-expressed in the cells together with APP-GFP, both the distance and the velocity further decreased to 149.2 ± 14.2 µm and 12.4 ± 0.9 µm/h, respectively (bellow single APP transfected cells). However, when we inhibited the catalytic activity of Cdc42, the values of both parameters under evaluation returned to GFP control cells' levels (254.1 ± 28.9 µm and 20.3 ± 0.9 µm/h).

Besides the total distance, the linear distance (the difference between the end and initial points) was also calculated (Figure 15). The linear distance migrated by cells increased as follows: APP-GFP+DsRed-Cdc42 wt (37.7 ± 4.1) < GFP (48.8 ± 7.2) < APP-GFP+DsRed-Cdc42 DN (60.8 ± 6.8) < APP-GFP (64.5 ± 5.3). These results confirm that, although APP expressing cells showed a decrease in the total distance migrated and velocity, they had an increased linear distance migrated, in agreement with a role in directed persistent migration. The catalytic activity of Cdc42 was highly detrimental for the migrated linear distance.

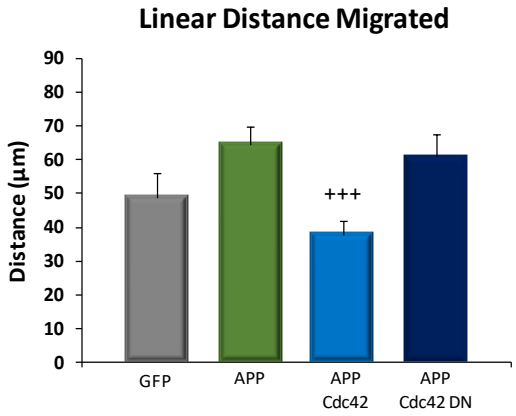

Figure 15. Average linear distance migrated by SH-SY5Y transfected cells in a SWH assay. Representative graph of average linear distance migrated by SH-SY5Y cells transfected with GFP (control), APP-GFP, or co-transfected with APP-GFP and DsRed-Cdc42 Wt or DN, in a scratch wound healing assay. The analysis was based on cells' X/Y coordinates, collected hourly for 13h, using the ImageJ software. Statistically significant difference, determined by the two-tailed unpaired t-test: +++p<0.001, for comparison between co-transfection with APP-GFP and DsRed-Cdc42 Wt condition and solely APP-GFP transfection (+).

2. Morphological Analysis of cells' polarization

In order to study the effects of APP and Cdc42 in the acquisition of the cells' migratory polarized phenotype, immunocytochemistry assays were performed.

In the first assay we transfected cells with GFP and APP-GFP and F-actin was labelled with the red fluorescent phalloidin. Figure 16 depicts transfected cells with migratory phenotype for both conditions.

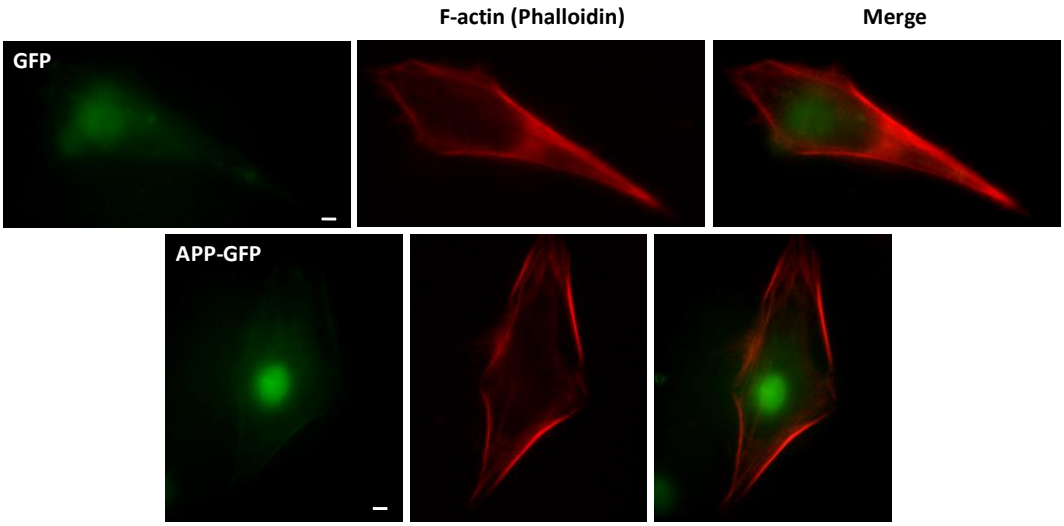

Figure 16. Migratory phenotype of GFP and APP-GFP expressing cells. Representative microphotographs of GFP and APP-GFP transfected cells. F-actin was labelled with red fluorescent phalloidin. Objective 100x. Scale bar - 10 µm.

In a second assay, APP expressing cells were co-transfected with both DsRed-Cdc42 Wt and DN, subject to immunocytochemistry procedures and cells-containing coverslips were mounted with a DAPI-containing medium. In Figure 17 we can see microphotographs of transfected cells for the conditions tested.

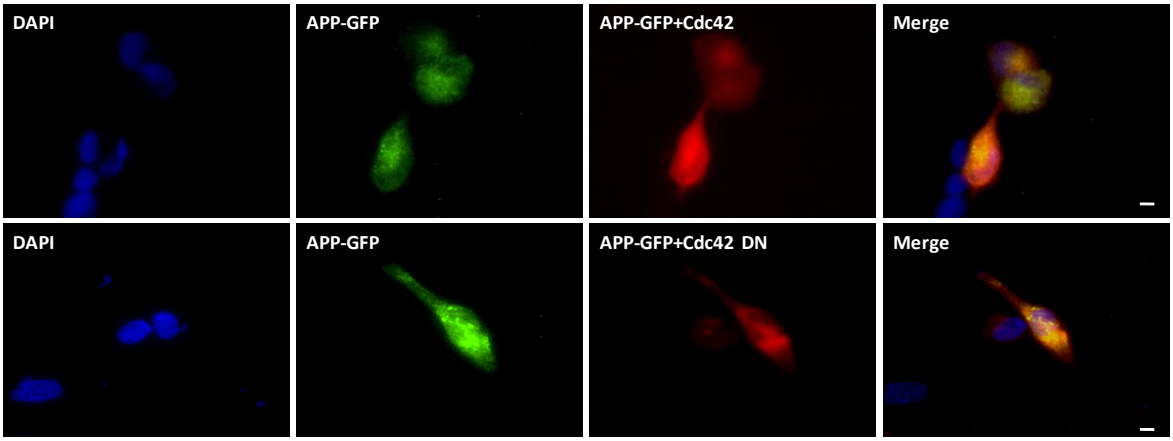

Figure 17. **Microphotographs of APP-GFP and DsRed-Cdc42 (DN and WT) co-transfected cells**. Analysis was performed by epifluorescence microscopy with fixed cells. Objective 20x. Bar - 10 µm.

The typical polarized phenotype, with asymmetric morphology and evident lamellipodia was analyzed, and the cells presenting this phenotype scored under an epifluorescence microscope with a 20x and a 100x objectives. Scores for the percentages of migratory transfected cells are presented in Figure 18.

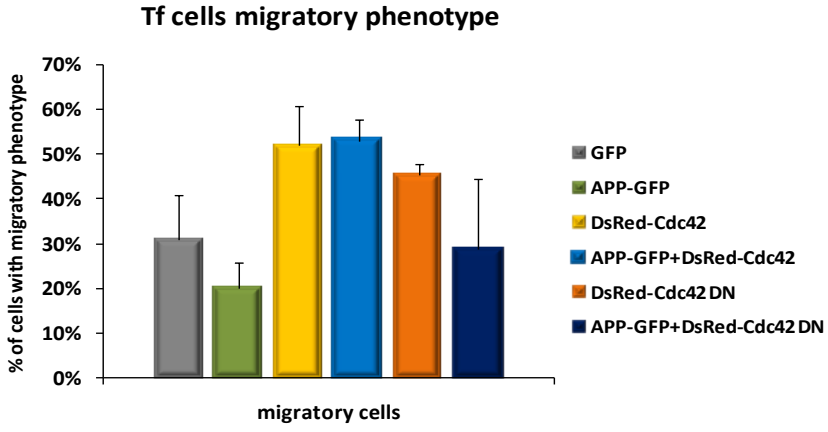

Figure 18. Percentage of migratory transfected cells. The number of SH-SY5Y transfected cells presenting a migratory phenotype was scored using epifluorescence microscopy. Cells were transfected for 17h with GFP (control) or APP-GFP Wt, alone or co-transfected with DsRed-Cdc42 Wt or DN cDNAs, N=2-3.

It was possible to see a slight decrease in the percentage of cells with migratory phenotype in APP transfected cells (20.1 ± 5.9% of the population) comparatively to the GFP transfected cells (31.1 ± 9.9%). Cells transfected with Cdc42 Wt alone (52.3 ± 8.6%) or co-transfected with Cdc42 Wt and APP (53.1 ± 4.9%) equally increased this morphology when compared with the two first conditions. The same was verified for cells transfected with Cdc42 DN alone (45.4 ± 2.6%). Co-transfection with APP-GFP and Cdc42 DN presented a small decrease relatively to all the other Cdc42 involving conditions, with a level very similar to the control (28.8 ± 15.7%), however more cells need to be analyzed to confirm these results.

3. APP role in F-actin dynamics

To find out the effect of APP on F-actin dynamics, a FRAP assay was performed on SH-SY5Y migrating cells co-transfected with LifeAct-RFP and either GFP or APP-GFP. Using a Sp5 Leica Confocal Microscope, the F-actin red fluorescence was photobleached at 2 specific ROIs per cell (front and rear) with the 561 nm laser at full power. A set of images was acquired before and after the photobleach (Figure 19).

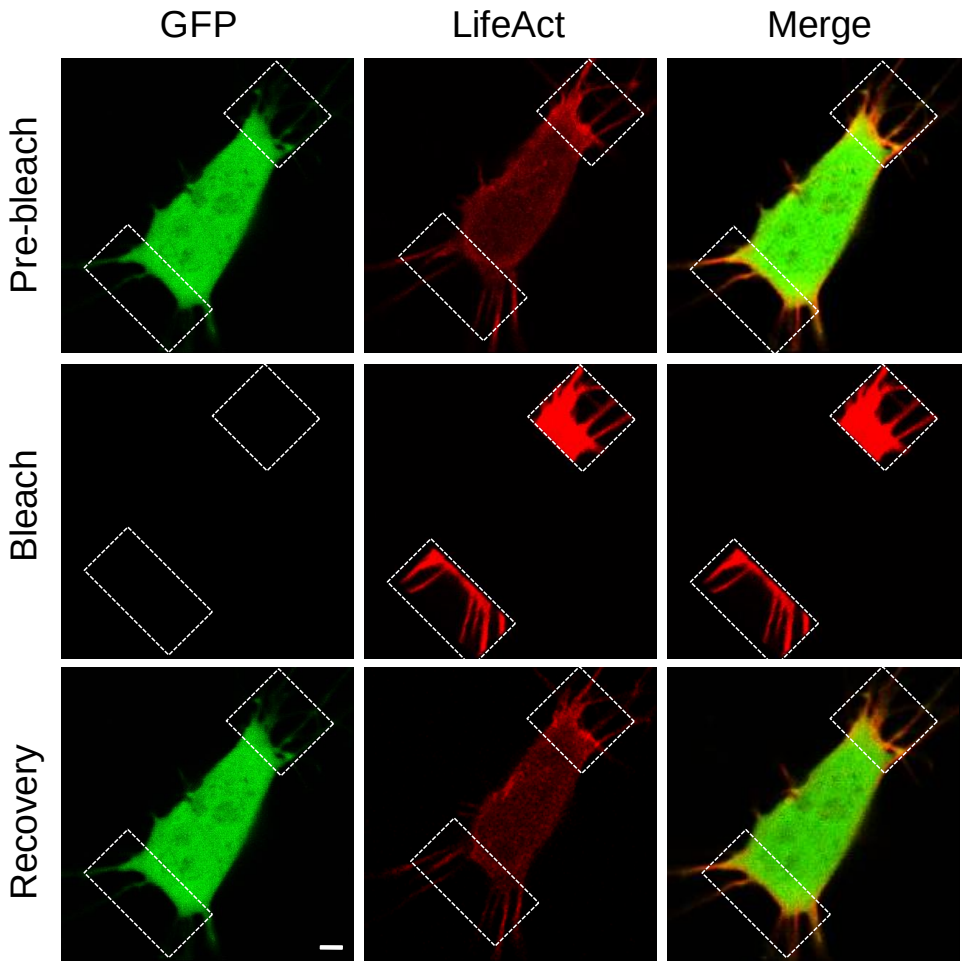

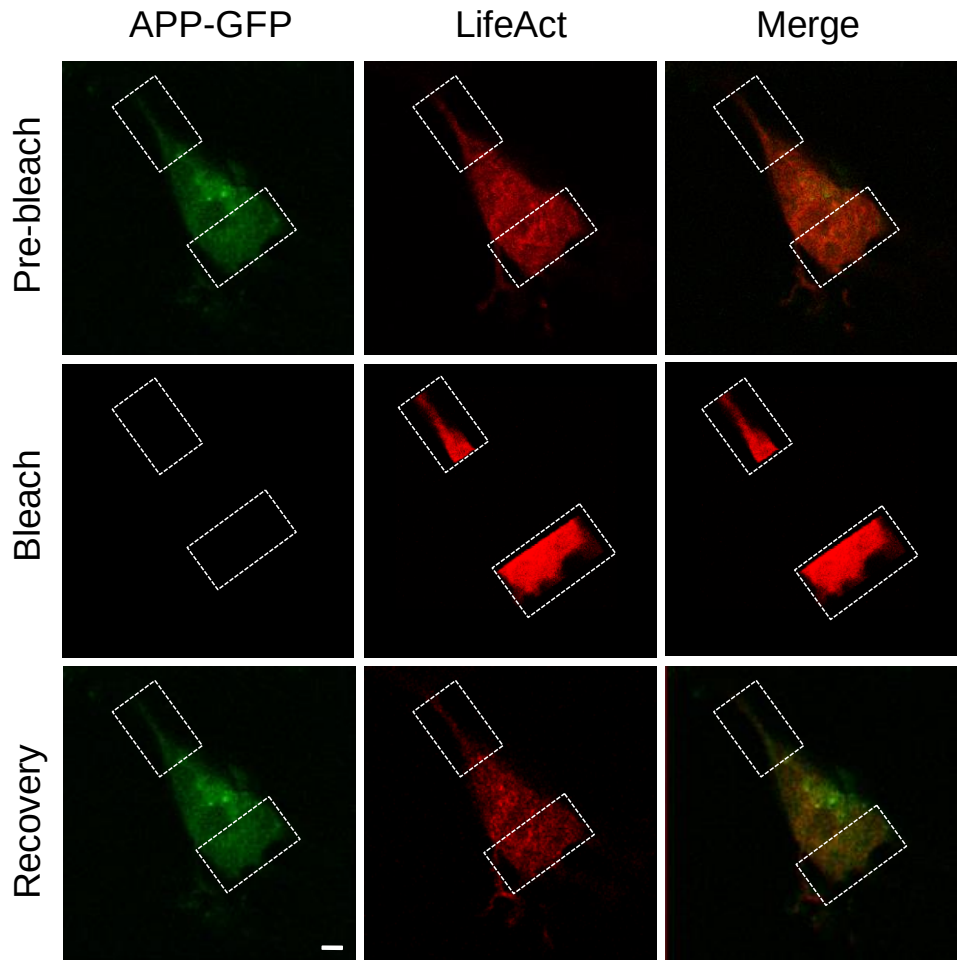

Figure 19. Microphotographs of sequential phases of a FRAP assay. Representative microphotographs of F-actin and GFP intensities in the pre-bleach, bleach and recovery phases of a FRAP analysis of SH-SY5Y cells co-transfected for 20h with LifeAct-RFP and GFP (upper panel) or the APP-GFP (lower panel), and subjected to a SWH assay. White boxes represent the two ROIs per cell that were chosen: cell front and rear. Scale bars - 10 µm.

Analyzing figure 19 we can see one cell of each condition in the different phases: prebleach, bleach and recovery phase. White boxes correspond to the selected ROI's (cell front and rear). Only the actin fluorescence was bleached, so the GFP fluorescence maintained the same. It is possible to qualitatively analyze the actin fluorescence intensity at the ROI's pre-bleach and after bleach. Often, they are not the same because the cells very hardly recover their initial fluorescence after the bleach. Using the LAS-AF software images were analysed and a FRAP curve was obtained for each bleached ROI of each cell (Figure 20).

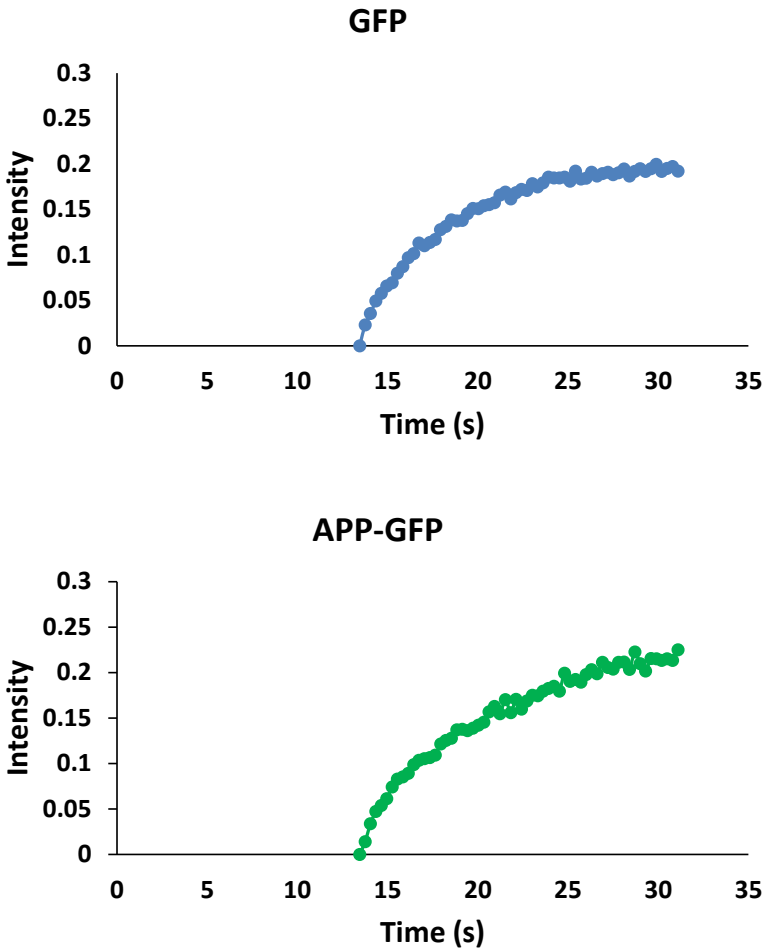

Figure 20. Intensity recover over time after photobleach on a FRAP assay. Exemplary graphs of recovery phase on a FRAP assay. Each graph corresponds to the cell rear of one cell of each condition (GFP and APP-GFP transfected cells) that represents the population analyzed. GFP (22 cells); APP-GFP (30 cells).

Based on that data, a quantitative analysis was performed and the average of all cells for the percentage and half-time of recovery were calculated for each ROI and for each condition (GFP control and APP transfected cells) (Figure 21).

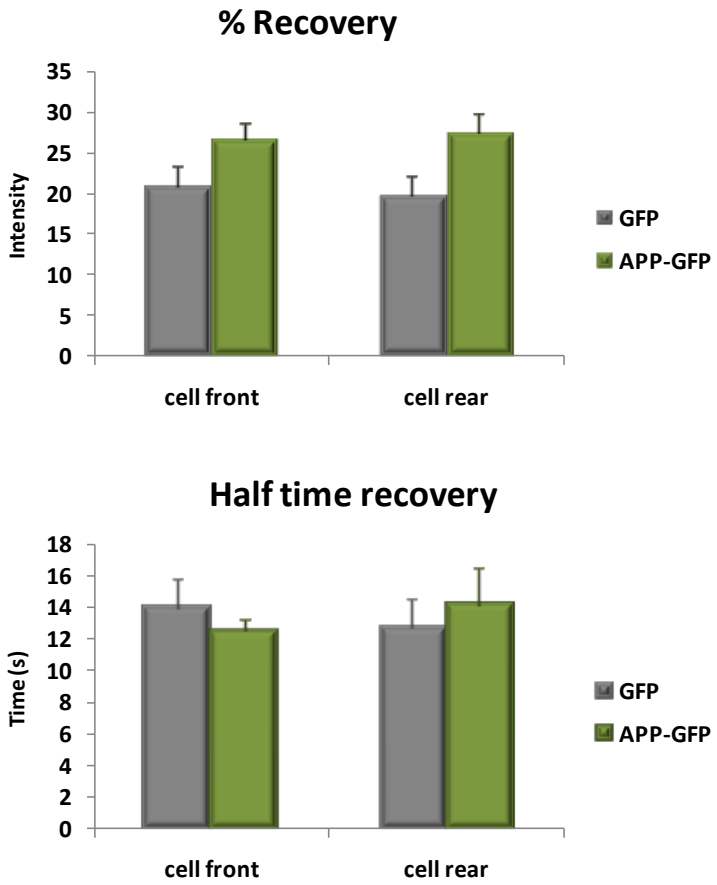

Figure 21. Fluorescence intensity recovery and corresponding time of GFP and APP-GFP transfected cells after photobleach in a FRAP assay. Representative graphs of percentage of recovery and half-time of recovery after photobleach of GFP (22 cells) and APP-GFP (30 cells) transfected cells subjected to a FRAP assay, (N=3).

It is possible to see some difference between the percentages of recovery of control cells (20.9 ± 2.2% at the front, 19.7 ± 2.1% at the rear) and APP transfected cells (26.7 ± 1.8% at the front, 27.4 ± 2.3% at the rear), with APP transfected cells tending to recover slightly more at both cell front and rear. APP does not seem to alter the rate of fluorescence intensity recover at both the cell front and the cell rear at least in these cells. To confirm an effect of APP on the percentage of recovery more cells need to be analysed.

Discussion

Studies silencing APP have already reported that neuronal precursor cells in embryonic cortex require APP to efficiently migrate to the nascent cortical plate [11]. Accumulating evidence supports the idea that APP is a cell-adhesion molecule that can interact with various binding partners and activate signalling pathways [10, 52]. The extracellular sequence of APP interacts with various extracellular matrix components, such as heparin, collagen type I and laminin, and with other APP N-terminal domains in transcellular interactions that promote cell-cell adhesion. The APP cytoplasmic domain, through binding to other proteins such as Fe65 and Mena, also participates in cell adhesion processes [51].

Together, APP and its interactor Fe65 help to regulate cell movement. Their co-expression greatly increased the positive effect of APP on cell movement, and together they accelerate wound closure in wound healing assays performed on MDCK cells. Another work has shown that, when together, these two proteins are involved in lamellipodia motility, as part of a larger macromolecular complex. Some of the effects of this macromolecular complex are mediated by Mena. Mena is an Abl-associated signalling protein involved in the regulation of actin dynamics in lamellipodia. APP and Fe65 colocalize with Mena and actin, and specifically concentrate with β1-integrin in nascent focal adhesions (FA; dynamic adhesion sites at the leading edge's lamellipodia) [38, 39].

Among other proteins involved in cell adhesion, there is the small GTPAse Cdc42. In a study performed in HeLa cells transfected with both Cdc42 Wt and DN, cells overexpressing Cdc42 Wt showed increased number of filopodia compared with the Cdc42 DN expressing cells (around the double) [44]. Active Cdc42 activates by its turn downstream targets of the WASP/WAVE family (WAVE2 for example), which activates the Arp2/3 complex. This complex regulates the formation of branches on actin filaments at the leading edge of migrating cells. Cdc42 is present in lamellipodia contributing to its extension and formation, acting essentially through formins [34]. Cdc42 also activates PAK that has a role in adhesion turnover [43].

The aims of this work were to analyse the role of APP in directed persistent migration and other migration parameters, its influence in the acquisition of a migratory morphology and in the stability of F-actin, in the SH-SY5Y

neuroblastoma cells. In addition, we sought to find out whether APP performs these functions independently, or together with the Cdc42 protein, especially with respect to the persistence in migration's direction.

In our lab we have previously observed that APP appeared to induce directed persistent migration in SH-SY5Y cells when compared to control cells. APP-GFP transfected cells were also observed to migrate slightly less and slower than GFP cells, although with a more defined trajectory [65]. Our results confirmed that APP overexpression induces directional persistent migration in SH-SY5Y cells, with APP transfected cells doubling the persistence in migration of control cells (figure 13). The linear migrated distance was also observed to be around 23% higher in APP-GFP expressing cells than in GFP (control) cells (figure 15), in contrast to the total distance migrated and the velocity, that decreased around 25% in APP-GFP transfected cells in comparison to GFP expressing cells (figure 14). With respect to the acquisition of a migratory phenotype, APP seems to decrease approximately 33% the number of cells with a polarized migratory morphology (figure 18). FRAP assays suggest that APP has a tendency to increase the pool of dynamic F-actin, although not significantly (figure 21).

When APP-GFP expressing cells also overexpressed Cdc42 Wt, the persistence in migration (figure 13) and the linear migrated distance (figure 15) were reduced to half of the values observed for solely APP-GFP overexpressing cells. The total migrated distance and the velocity (figure 14) were also impaired by around 25% with the co-overexpression of catalytically active Cdc42. On the other hand, the migratory phenotype acquisition was higher in both these cells (53%) and in solely Cdc42 Wt expressing cells (52%), when compared with solely APP-GFP expressing cells (20%) (figure 18).

When a catalytic dead Cdc42 was co-overexpressed with APP (co-transfection with Cdc42 DN), the persistence in migration improved 25% (the out of track percentage reduced from 334% to 256%) when compared with APP-GFP+DsRed-Cdc42 wt co-expressing cells, although being still 50% less persistent than APP-GFP expressing cells (174%) (figure 3). The total migrated distance and velocity returned to levels very similar to control (GFP expressing) cells, being slightly higher than APP-GFP expressing cells (figure 14). The lower persistence but

higher velocity resulted in a linear migrated distance for APP-GFP+DsRed-Cdc42 DN equal to the one observed for solely APP-GFP expressing cells (figure 15). In what concerns the migratory phenotype, DsRed-Cdc42 DN alone did not impair the acquisition of polarized morphology, but the co-expression of APP-GFP and Cdc42 DN slightly reduced the number of cells observed with this phenotype (figure 18).

The decrease in total migrated distance (and related velocity parameter) observed for APP-GFP expressing cells (figure 14) may be explained by the known roles of APP such as its interaction with Mena and β1-integrin, that in turns activates FAK. These proteins are found in nascent FA and contribute to cell adhesion, in this way reducing the ability of cells to migrate faster [68]. Further, the increased adhesion may give cells the time to have a more linear migration. In addition, Mena has a role in regulating cell protrusion and migration by controlling actin filament branching at the leading edge, and to activate profilin that participates in the actin treadmilling, in this way contributing to a more persistent direction of migration, with few detours of the original track [68]. APP may thus be increasing cell's persistence in direction through Mena, but not through Cdc42, since the presence of constitutively active Cdc42 worsen not only the total distance migrated and the velocity, but also the linearity and persistence of migration. Cdc42 coordinates several proccesses involved in cell polarity and migration [70]. For example, it has a known role both in the formation of filopodia and in the activation of Arp2/3 via WASP activation. Activated Arp2/3 regulates F-actin branching in lamellipodia and locates in nascent FAs, leading to the formation of lamellipodia and larger nascent FAs. The increased adhesion of cells to the substrate slows down cells migration, thus reducing its total distance and velocity, as observed for APP-GFP and DsRed-Cdc42 Wt overexpressing cells. When the activity of the overexpressed Cdc42 was abolished, the cell adhesion pathways activated by Cdc42 were also inhibited, and cells recovered the ability to migrate faster, less attached. Importantly, APP and Cdc42 overexpression promoted APP's negative effect on cells' velocity, while APP co-expression with Cdc42 DN annuled this APP effect (figure 14). We thus hypothesize that APP may be activating Cdc42 [65], which in turns activates WASP to activate Arp2/3, which

interacts with FAK and vimentin (adhesion molecules), promoting the assembly of new nascent FAs, and resulting in a more stable, although dynamic, leading edge [69].

The co-overexpression of APP with either Cdc42, Wt or DN, decreased persistence in migration, with catalytically active Cdc42 Wt completely annulling the APP effect (figure 13). Yamao *et al*., showed that native Cdc42 probably has a function in randomly cell migration [41]. Further, it is known that Cdc42 activates PAK, a kinase that promotes the actin turnover of mature focal adhesions. This actin turnover increases the shift between disassembly of already formed focal adhesions and assembly of new nascent adhesions. We hypothesize that this turnover, together with increased formation of filopodia at the leading edge and surreoundings, may cause the cell's loss of persistence in directed migration. Indeed, in the APP-GFP and Cdc42 DN overexpressed cells, these did not migrate as randomly as the cells that overexpressed APP-GFP and Cdc42 Wt, but they were also not as targeted as the cells that only overexpressing APP-GFP (figures 12, 13 and 15). It is possible that the excessive Cdc42 (even catalitically dead) binds and recruits APP out of nascent focal adhesions. On the other hand, Cdc42, both Wt and DN, are involved in the formation of filopodia, although this is more evident in Wt form. Therefore, and also due to the role of Cdc42 in the activation of PAK and consequent increase of turnover of FAs, there may be a higher loss of direction in cells co-expressing APP-GFP and Cdc42 Wt than in those that co-express APP-GFP and Cdc42 DN.

With our results we conclude that APP does not induce persistence of migration through Cdc42. APP can activate Cdc42 [65], causing the increase of adhesion as explained above, and thus leading to a decrease in the distance and velocity of migration, but since Cdc42 worsens the effect of APP on persistence, it acts independently of Cdc42 in this parameter. In addition, we hypothesize that APP may be inducing the persistence of migration by other means. This may include Mena, as observed above, but also for example, PTP1B. This is a non-receptor tyrosine phosphatase bound to the cytosolic face of the ER through a hydrophobic C-terminal tail. PTP1B is present in complexes with β1 and β3-integrin and interacts with an adaptor protein, p130Cas, which in part localizes at

focal adhesions. Burdisso, *et al*., suggested PTP1B as a contributing protein to anchor new adhesions to the actin cytoskeleton during protrusions. In this study they demonstrated that paxilin adhesions targeted with the ER tubules containing PTP1B extended by approximately fivefold their lifetimes compared to those not targeted, or targeted with ER tubules bearing inactive PTP1B. The authors also demonstrated that PTP1B KO cells had increased turnover of Fas, and decreased directionality, suggesting a role for PTB1B in increased stabilizations and lifetime of adhesions, and in promoting direction of migration. Thus, we hypothesize that, once PTP1B forms complexes with β1 integrin, that also interacts with APP, the amyloid precursor protein may also be acting in the persistence of migration through activation/interaction with this phosphatase [71].

Regarding cells's polarization in SH-SY5Y cellls, APP has few effect, showing a tendency to decrease the acquisition of polarization, in opposite to the increase in this parameter for solely Cdc42 transfected cells (figure 18). We observed an increased number of polarized cells in APP-GFP+DsRed-Cdc42 wt co-transfection and in solely Cdc42 transfection, partially due to the above described role of Cdc42 in the formation of filopodia, besides its activation of PAR. Second, the Cdc42 molecule per se, even when inactive, increased cell polarization (single Cdc42 DN transfected cells). It seems that the catalytic activity of Cdc42 is important for polarization, but the presence of Cdc42 as an interactor molecule seems more important. Still, when co-transfected with APP, the amyloid precursor protein may be interacting with Cdc42 and deviating it from pathways such as the PAR complex pathway, which contributes to polarization. APP would thus reduce the number of cells with migratory phenotype in the APP-GFP+DsRed-Cdc42 DN condition; also, APP may be sequestering some Cdc42 out of the filopodias. This APP effect is apparent in the APP-GFP+DsRed42 DN condition, but not in the APP-GFP+DsRed-Cdc42 Wt, probably because the catalytic activity of Cdc42 counter balances the sequestering role of APP. However, these conditions were only tested twice, and the number of biologic replicas needs to increase for conclusions to be taken.

Finally, APP seems to induce more dynamic to the F-actin population (figure 21), although more work needs to be performed to prove it. If true, this is probably

resulting from the potential APP-induced activation of Arp 2/3 via Cdc42, and from APP interaction with Mena, a protein that activates profilin leading to increase actin treadmilling. Also, if APP activates the endogenous Cdc42, this may also activate signalling pathways that lead to the actin turnover, via PAK, for example. To confirm this hypothesis, FRAP assays of Cdc42 Wt and DN, together with APP or alone, must be performed.

Conclusion

This work allowed us to understand the influence of APP in several migratory processes and its interaction with the Cdc42 protein. It was possible to confirm that APP positively influences persistent directed migration of SH-SY5Y cells independently of Cdc42, but to observe that APP decreases the total distance and velocity of migrations of these cells, with the small GTPase Cdc42 worsens these parameters.

It was also possible to conclude that APP alone has no significant influence on the polarization of cells, whereas Cdc42, both the active and the DN form, increased the number of cells with migratory phenotype. In the Cdc42 Wt conditions the number of cells with migratory phenotype is not influenced by the overexpression of APP-GFP. The same was not observed for Cdc42 DN conditions, where the overexpression of APP and Cdc42 DN together seemed to reduce the number of migratory cells in the population.

Last but not least, is was possible to see atendency for APP to increase the dynamic F-actin population at the cell rear and leading edge of migrating cells in SH-SY5Y cells.

As future prespectives, we intend to repeat ICC assays to confirm the role of Cdc42 and APP in polarization; score the number of filopodia in APP-GFP and APP-GFP+Cdc42 conditions; increase the number of FRAP assays to draw more precise conclusions about the influence of APP on the dynamics of F-actin and also include co-transfections with Cdc42 in this experiment to explore its influence in this process. We also plan to perform co-localization studies of APP with endogenous and exogenous Cdc42, and to prove that APP interacts with active and inactive Cdc42.

References

[1] Zhou, Z., Chan, C. H., Ma, Q., Xu, X., Xiao, Z., & Tan, E. (2011). The roles of amyloid precursor protein (APP) in neurogenesis, implications to pathogenesis and therapy of Alzheimer disease (AD), 5(4), 280–292. *doi*:10.4161/cam.5.4.16986

[2] Nicolas, M., & Hassan, B. A. (2014). Amyloid precursor protein and neural development, 2543–2548. *doi*:10.1242/dev.108712

[3] Chen, Y., & Tang, B. L. (2006). The amyloid precursor protein and postnatal neurogenesis/neuroregeneration, 341, 1–5. *doi*: 10.1016/j.bbrc.2005.12.150

[4] O'Brien RJ, Wong PC. Amyloid Precursor Protein Processing and Alzheimer's Disease. Annual review of neuroscience. 2011; 34:185-204. *doi*: 10.1146/annurev-neuro-061010-113613

[5] Haass, C., Kaether, C., Thinakaran, G., & Sisodia, S. (2012). Trafficking and Proteolytic Processing of APP, 1–25. *doi*: 10.1101/cshperspect.a006270

[6] Small, S. A., & Gandy, S. (2006). Sorting through the Cell Biology of Alzheimer's Disease : Intracellular Pathways to Pathogenesis, 15–31. *doi*: 10.1016/j.neuron.2006.09.001

[7] Jiang, S., Li, Y., Zhang, X., Bu, G., Xu, H., & Zhang, Y. (2014). Trafficking regulation of proteins in Alzheimer's disease, 1–13. *doi*: 10.1186/1750-1326-9-6

[8] Ando, K., Oishi, M., Takeda, S., Iijima, K., Isohara, T., Nairn, A. C., Kirino, Y., Greengard, P., & Suzuki, T. (1999). Role of Phosphorylation of Alzheimer's Amyloid Precursor Protein during Neuronal Differentiation, 19 (11), 4421–4427. *doi*: 10.1523/JNEUROSCI.19-11-04421.1999

[9] Walter, J., Capell, A., Hung, A. Y., Langen, H., Schno, M., Thinakaran, G., Sisodia, S. S., Selkoe, D. J., & Haass, C. (1997). Ectodomain Phosphorylation

of β-Amyloid Precursor Protein at Two Distinct Cellular Locations, 272(3), 1896–1903. *doi*: 10.1074/jbc.M002850200

[10] Deyts, C., Thinakaran, G., & Parent, A. T. (2016). Review APP Receptor ? To Be or Not To Be, xx, 1–22. doi: 10.1016/j.tips.2016.01.005

[11] Young-pearse, T. L., Bai, J., Chang, R., Zheng, J. B., Loturco, J. J., & Selkoe, D. J. (2007). A Critical Function for β-Amyloid Precursor Protein in Neuronal Migration Revealed by In Utero RNA Interference, 27 (52), 14459–14469. *doi*: 10.1523/JNEUROSCI.4701-07.2007

[12] Pastorino, L., & Lu, K. P. (2004). Phosphorylation of the Amyloid Percursor Protein (APP): Is this a mechanisms in favor or against Alzheimer Disease?, 35(3). *doi*: 10.1002/nrc.20035

[13] Vieira, S.I., Rebelo, S., Domingues, S. C., Edgar, Da Cruz e Silva, E.S., & Da Cruz e Silva, O. A. B. (2009). S655 phosphorylation enhances APP secretory traffic. *Mol. Cell. Biochem.* 328:145-54. *doi*: 10.1007/s11010-009-0084-7.

[14] Vieira, S. I., Rebelo, S., Esselmann, H., Wiltfang, J., Lah, J., Lane, R., Small, S.A., Gandy, S., Da Cruz e Silva, E.F., & Da Cruz e Silva, O.A.B. (2010). Retrieval of the Alzheimer's amyloid precursor protein from the endosome to the TGN is S655 phosphorylation state-dependent and retromer-mediated, 1–21. *doi*: 10.1186/1750-1326-5-40

[15] Ming, G., & Song, H. (2011). Review Adult Neurogenesis in the Mammalian Brain : Significant Answers and Significant Questions. Neuron, 70 (4), 687–702. *doi*: 10.1016/j.neuron.2011.05.001

[16] Ming, G., & Song, H. (2005). Adult Neurogenesis in the Mammalian Central Nervous System. doi: 10.1146/annurev.neuro.28.051804.101459

[17] Liu, C., & Zhao, Æ. X. (2009). MicroRNAs in Adult and Embryonic Neurogenesis, 141–152. *doi*: 10.1007/s12017-009-8077-y

[18] Ohsawa, I., Takamura, C., Morimoto, T., Ishiguro, M., & Kohsaka, S. (1999). Amino-terminal region of secreted form of amyloid precursor protein

stimulates proliferation of neural stem cells, 11, 1907–1913. *doi*: 10.1046/j.1460-9568.1999.00601.x

[19] Caillé, I., Allinquant, B., Dupont, E., Bouillot, C., Langer, A., Müller, U., & Prochiantz, A. (2004). Soluble form of amyloid precursor protein regulates proliferation of progenitors in the adult subventricular zone. *doi*: 10.1242/dev.01103

[20] Baratchi, S., Evans, J., Tate, W. P., Abraham, W. C., & Connor, B. (2011). Secreted Amyloid Precursor Proteins Promote Proliferation and Glial Differentiation of Adult Hippocampal Neural Progenitor Cells, (September). *doi*: 10.1002/hipo.20988

[21] Goodman, Y., & Mattson, M.P. (1994). Secreted Forms of β-Amyloid Precursor Protein Protect Hippocampal Neurons against Amyloid β-Peptide-Induced Oxidative Injury, Experimental Neurology, 128(1), 1-12. *doi*: 10.1006/exnr.1994.1107

[22] Ma, Quang-H., Futagawa, T., Yang, W., Jiang, Xiao., Zeng, Li., Takeda, Y., Xu, R., Bagnard, D., Schaschner, M., Furley, A., Karagogeos, D., Wtanabe, K., Dawe, G. and Xiao, Z. (2008). A TAG1-APP signalling pathway through Fe65 negatively modulates neurogenesis, 10 (3). *doi*: 10.1038/ncb1690

[23] Ghosal, K., Stathopoulos, A., & Pimplikar, S. W. (2010). APP Intracellular Domain Impairs Adult Neurogenesis in Transgenic Mice by Inducing Neuroinflammation, 5 (7). *doi*: 10.1371/journal.pone.0011866

[24] Yoshikawa, K., Aizawa, T., & Hayashi, Y. (1992). Degeneration in vitro of post-mitotic neurons overexpressing the Alzheimer amyloid protein percursor. Letters to Nature. 359 (3). *doi*: 10.1038/359064a0

[25] Haughey, N. J., Liu, D., Nath, A., Borchard, A. C., & Mattson, M. P. (2002). Disruption of Neurogenesis in the Subventricular Zone of Adult Mice, and in Human Cortical Neuronal Precursor Cells in Culture, by Amyloid β-Peptide, 1, 125–135. *doi*: 10.1385/NMM:1:2:125

[26] Lo, M. A., & Shelanski, M. L. (2004). Neurogenic Effect of β-Amyloid Peptide in the Development of Neural Stem Cells, 24 (23), 5439–5444. *doi*: 10.1523/JNEUROSCI.0974-04.2004

[27] Sotthibundhu, A., Li, Q., Thangnipon, W., & Coulson, E. J. (2009). Aβ $_{1-42}$ stimulates adult SVZ neurogenesis through the p75 neurotrophin receptor, 30, 1975–1985. *doi*: 10.1016/j.neurobiolaging.2008.02.004

[28] Lazarov, O., & Michael, P. (2012). All in the family : how the APPs regulate neurogenesis, 6 (June), 1–21. *doi*: 10.3389/fnins.2012.00081

[29] Coronel, R., Bernabeu-zornoza, A., Palmer, C., Muñiz-moreno, M., Zambrano, A., Cano, E., & Liste, I. (2018). Role of Amyloid Precursor Protein (APP) and Its Derivatives in the Biology and Cell Fate Specification of Neural Stem Cells. *doi*: 10.1007/s12035-018-0914-2

[30] Clainche, C. L. E., & Carlier, M. (2008). Regulation of Actin Assembly Associated With protrusion and Adhesion in Cell Migration, 489–513. *doi*: 10.1152/physrev.00021.2007

[31] Schaar, B. T., & Mcconnell, S. K. (2005). Cytoskeletal coordination during neuronal migration, 2005. *doi*: 10.1073/pnas.0506008102

[32] Kaneko, K., Sawada, M., & Sawamoto, K. (2017). Mechanisms of neuronal migration in the adult brain, 0–3. *doi*: 10.1111/jnc.14002

[33] Turner, K. L., & Sontheimer, H. (2014). KCa3.1 Modulates Neuroblast Migration Along the Rostral Migratory Stream (RMS) In Vivo, (September), 2388–2400. *doi*: 10.1093/cercor/bht090

[34] Kurosaka, S., & Kashina, A. Manuscript, A. (2008). Cell Biology of Embryonic Migration, 84 (2). 102-122. *doi*: 10.1002/bdrc.20125.

[35] Coles, C. H., & Bradke, F. (2015). Review Coordinating Neuronal Actin – Microtubule Dynamics. Current Biology, 25(15), R677–R691. *doi*: 10.1016/j.cub.2015.06.020

[36] Ridley, A. J. (2012). Cell Migration : Integrating Signals from, 1704(2003). *doi*: 10.1126/science.1092053

[37] Lauffenburger, D. A., & Horwitz, A. F. (1996). Cell Migration : A Physically Integrated Molecular Process, 84, 359–369. *doi*: 10.1016/S0092-8674(00)81280-5

[38] Sabo, S. L., Ikin, A. F., Buxbaum, J. D., & Greengard, P. (2001). The Alzheimer Amyloid Precursor Protein (APP) and FE65, an APP-binding Protein, Regulate Cell Movement, 153(7), 1403–1414. *doi*: 10.1083/jcb.153.7.1403

[39] Copenhaver, P. F., & Ramaker, J. M. (2017). Neuronal Migration during development and the Amyloid Percursor Protein, 1–10. doi: 10.1016/j.cois.2016.08.001

[40] Ridley, A. J. (2015). Rho GTPase signalling in cell migration. *Current Opinion in Cell Biology*, *36*, 103–112. doi: 10.1016/j.ceb.2015.08.005

[41] Yamato, M., Naoki, H., Kunida, K., & Aoki, K. (n.d.). Distinct predictive performance of Rac1 and Cdc42 in cell migration. *Nature Publishing Group*, 1–14. *doi*: 10.1038/srep17527

[42] Kurisu, S., & Takenawa, T. (2010). WASP and WAVE family proteins : Friends or foes in cancer invasion, *101*(10), 2093–2104. *doi*: 10.1111/j.1349-7006.2010.01654.x

[43] Rane, C. K., Minden, A., Rane, C. K., & Minden, A. (2014). P21 activated kinases Structure , regulation , and functions, *1248*. *doi*: 10.4161/sgtp.28003

[44] Ye, H., Zhang, Y., Geng, L., & Li, Z. (2015). Cdc42 expression in cervical cancer and its effects on cervical tumor invasion and migration, 757–763. *doi*: 10.3892/ijo.2014.2748

[45] Vadodaria, K. C., Brakebusch, C., Suter, U., & Jessberger, S. (2013). Stage-Specific Functions of the Small Rho GTPases Cdc42 and Rac1 for Adult Hippocampal Neurogenesis, *33*(3), 1179–1189. *doi*: 10.1523/JNEUROSCI.2103-12.2013.

[46] Etienne-manneville, S. (2002). Rho GTPases in cell biology, *420*(December), 629–635. *doi*: 10.1038/nature01148

[47] Cappello, S., et al (2006). The Rho-GTPase cdc42 regulates neural progenitor fate at the apical surface, *9*(9), 1099–1107. *doi*: 10.1038/nn1744

[48] Petrie, R. J., Doyle, A. D., & Yamada, K. M. (2010). The Rho GTPAse cdc42 regulates neural progenitor fate at the apical surface, *10*(8), 538–549. *doi*: 10.1038/nn1744

[49] Raftopoulou, M., & Hall, A. (2004). Cell migration : Rho GTPases lead the way, *265*, 23–32. *doi*: 10.1016/j.ydbio.2003.06.003

[50] Stiles, J., & Jernigan, T. L. (2010). The Basics of Brain Development, 327–348. *doi*: 10.1007/s11065-010-9148-4

[51] Mu, U. C. (2012). Physiological Functions of APP Family Proteins, (2), 1–17. *doi*: 10.1101/cshperspect.a006288

[52] Zhang, H., Ma, Q., Zhang, Y. and Xu, H. (2013).Proteolytic Processing of Alzheimer's β-amyloid precursor protein, *120* (Suppl 1), 9–21. *doi*: 10.1111/j.1471-4159.2011.07519.x

[53] Anderson, L. R., Owens, T. W., & Naylor, M. J. (2014). Structural and mechanical functions of integrins. *Biophysical Reviews*, *6*(2), 203–213. *do*i: 10.1007/s12551-013-0124-0

[54] Kozma, R., Ahmed, S., Best, A., & Lim, L. (1995). The Ras-related protein Cdc42Hs and bradykinin promote formation of peripheral actin microspikes and filopodia in Swiss 3T3 fibroblasts. *Molecular and Cellular Biology*, *15*(4), 1942–1952. *doi*: 10.1128/MCB.15.4.1942

[55] Nobes, C. D., & Hall, A. (1995). Rho, Rac, and Cdc42 GTPases regulate the assembly of multimolecular focal complexes associated with actin stress fibers, lamellipodia, and filopodia. *Cell*, *81*(1), 53–62.

[56] Czuchra, A. Wu, X., Meyer, H., Hengel, J., Schroeder, T., Geffers, R., Rottner, K. and Brakebusch, C. (2005). Cdc42 Is Not Essential for Filopodium Formation, Directed Migration, Cell Polarization, and Mitosis in Fibroblastoid Cells. *doi*: 10.1091/mbc.e05-01-0061

[58] Alleaume, C., Eychène, A., Harnois, T., Bourmeyster, N., Constantin, B., Caigneaux, E., Philippe, M. (2004). Vasoactive intestinal peptide-induced neurite remodeling in human neuroblastoma SH-SY5Y cells implicates the Cdc42 GTPase and is independent of Ras-ERK pathway. *Experimental Cell Research*, *299*(2), 511–524. *doi*: 10.1016/j.yexcr.2004.06.016

[59] Fluorescence Recovery after Photo Bleaching (FRAP) [internet]. 2011. Available at: https://www.leica-microsystems.com/science-lab/fluorescence-recovery-after-photobleaching-frap-and-its-offspring/

[60] Quantitative Fluorescence: An overview [Internet]. 2012. Available at: https://www.leica-microsystems.com/science-lab/quantitative-fluorescence/

[61] Pankov, R., Endo, Y., Even-Ram, S., Araki, M., Clark, K., Cukierman, E., … Yamada, K. M. (2005). A Rac switch regulates random versus directionally persistent cell migration. *Journal of Cell Biology*, *170*(5), 793–802. *doi*: 10.1083/jcb.200503152

[62] Halftime. EAMNET-FRAP module. [Internet]. 2004. Available at: https://www.embl.de/eamnet/frap/html/halftime.html

[63] Matsumoto, K., Akao, Y., Yi, H., Shamoto-Nagai, M., Maruyama, W., & Naoi, M. (2006). Overexpression of amyloid precursor protein induces susceptibility to oxidative stress in human neuroblastoma SH-SY5Y cells. *Journal of Neural Transmission*, *113*(2), 125–135. *doi*: 10.1007/s00702-005-0318-0

[64] Mayor, R., & Carmona-Fontaine, C. (2010). Keeping in touch with contact inhibition of locomotion. *Trends in Cell Biology*, *20*(6), 319–328. *doi*: 10.1016/j.tcb.2010.03.005

[65] Pinho, A.C.D. de. (2012). Unveiling the APP role in cell migration. Repositório Institucional – Secção Autónoma de Ciências da Saúde da Universidade de Aveiro

[66] da Rocha, J.; da Cruz e Silva, O.A.B and Vieira, S.I. (2015). Analysis of the amyloid precursor protein role in neuritogenesis reveals a biphasic SH-SY5Y neuronal cell differentiation model. *Journal of Neurochemistry*. 134, 288-301. *doi*: 10.1111/jnc.13133

[67] Public Health England. (2017). Cell Line Profile MDA-MB-231, (94030304), 3. Retrieved from https://www.phe-culturecollections.org.uk/media/133182/mda-mb-231-cell-line-profile.pdf

[68] Wozniak, M. A., Modzelewska, K., Kwong, L., & Keely, P. J. (2004). Focal adhesion regulation of cell behavior. *Biochimica et Biophysica Acta - Molecular Cell Research*, *1692*(2–3), 103–119. *doi*:10.1016/j.bbamcr.2004.04.007

[69] Huttenlocher, A., & Horwitz, A. R. (2011). Integrins in Cell Migration, 1–16. d*oi*:10.1101/cshperspect.a005074

[70] Etienne-Manneville, S. (2004). Cdc42 - the centre of polarity. *Journal of Cell Science*, *117*(8), 1291–1300. *doi*:10.1242/jcs.01115

[71] Burdisso, J. E., Gonzalez, A., & Arregui, C. O. (2013). PTP1B promotes focal complex maturation, lamellar persistence and directional migration. *Journal of Cell Science*, *126*(8), 1820–1831.*doi*:10.1242/jcs.118828

Appendix

cDNA amplification solutions

1.1. Luria-Bertani (LB) growth medium with Ampicilin/Kanamicin

For a final volume of 1 L, dissolve 25 g of LB Broth (nzytech) in deionized water (dH_2O). Adjust the volume up to 1 L of dH_2O and autoclave the solution (the LB will mix during autoclaving). Let the medium cool down to 60ºC and add 1 mL of ampicilin of a 50 mg/mL stock or 1 mL of kanamicin of a 30 mg/mL stock solution (optional). Store at 4ºC.

1.2. LB /Agar plates with Apicilin/Kanamicin

For a final volume of 1L, dissolve 25g of LB Broth, and 12g of Agar in deionized water (dH_2O). Adjust the volume up to 1L of dH_2O and autoclave the solution. Let the medium cool down to 60ºC and add 1mL of ampicilin of a 50mg/mL stock or 1mL of Kanamicin of a 30mg/mL stock solution. Drop approximately 20ml per plate, let solidify at room temperature and store the plates with the lid facing down, in a bag closed at 4º.

2. Competent cells protocol solutions

2.1. Solution I

For a final volume of 500 mL:

- 75 g of glycerol;
- 4,95 g of $MnCl_2 \cdot 4H_2O$;
- 0,75 g of $CaCl_2 \cdot 2H_2O$;
- 3 mL of KAc 5M;
- Adjust pH with HCl until 5,8;
- Filter the solution.

2.2. Solution II

For a final volume of 500mL:

- 75 g of glycerol;
- 10 mL of MOPS 0,5M;
- 0,6 g of RbCl;
- 5,5 g of $CaCl_2 \cdot 2H_2O$;
- Filter the solution.

2.3. SOB medium

For a final volume of 1 L dissolve 25,5 g of SOB Broth (nzytech) in deionized water (dH_2O). Add 10 mL of Kl 250 mM. Adjust pH until 7 with NaOH. Adjust the volume until 1 L with dH_2O. Autoclave the solution. Before use, add 5 mL of $MgCl_2$ 2M and 5 mL of $MgSO_4$ 2M.

3. Miniprep solutions

3.1. Solution I

- Glucose 50 mM;
- Tris-Cl (ph 8.0) 25 mM;
- EDTA (ph 8.0) 10 mM

Autoclave for 15 minutes.

3.2. Solution II

- NaOH 0,2 N (diluted fresh from a 10 N stock;
- SDS 1% (m/v);

Prepare right before use, and use it at room temperature.

3.3. Solution III

- Potassium acetate 5 M, 60 mL;
- Glacial acetic acid 11,5 mL;
- dH_2O 28,5 mL

Store at 4ºC, place on ice before use.

EDTA

To prepare 0.5M EDTA (pH8.0): Add 186.1g of disodium salt EDTA • 2 H_2O to 800ml of dH_2O. Shake vigorously using a magnetic stirrer. Set PH to 8.0 with NaOH (around 20 g NaOH). Aliquot and sterilize by autoclaving. The salt disodium solution can not dissolve until the pH of the solution is adjusted to approximately 8.0.

NaOH

The preparation of 10N NaOH involves an extremely exothermic reaction, which can lead to breakage of glass material, and is then prepared with extreme caution in plastic graduated cups. To 800ml of dH_2O, add slowly and drop by drop 400g of NaOH tablets, stirring constantly. As an additional precaution, place the glass on ice. When the tablets are fully dissolved adjust the volume to 1L with dH_2O. Store the solution in a plastic bottle room temperature. It is not necessary to sterilize.

SDS

To prepare a 20% (w/v) solution, dissolve 200g of electrophoresis grade SDS in 900ml dH_2O. Heat to 68ºC and stir using a magnetic stirrer. If necessary adjust the pH to 7.2 by adding a few drops of concentrated HCl. Adjust the volume to 1 liter with dH_2O. If at room temperature, it is not necessary to sterilize. Do not autoclave.

Tris-Cl (1M)

Dissolve 121.1g of Tris base in 800ml of dH_2O. Adjust the pH to the desired value by adding concentrated HCl: HCl (70, 60, 42 mL) should have respective pH (7.4, 7.6, 7.8). Allow the solution to cool to room temperature before final pH

adjustment. Adjust the volume of the solution to 1 liter with dH_2O. Aliquot and sterilize by autoclaving. Discard the 1M solution if it has a yellow color (indicative that the Tris is not of the desired quality). The pH of Tris solutions is temperature dependent and decreases approximately 0.03 pH units per 1ºC increase in temperature. For example, a 0.05M solution has pH values 9.5, 8.9, and 8.6 at 5˚C, 25˚C, and 37˚C, respectively.

4. Cell Culture and Immunocytochemistry Solutions

4.1. PBS (1x)

For a final volume of 500mL, dissolve one pack of BupH Modified Dulbecco's Phosphate Buffered Saline Pack (Pierce) in deionized H_2O. Final composition:

- 8 mM Sodium Phosphate;
- 2 mM Potassium Phosphate;
- 140 mM Sodium Chloride;
- 10 mM Potassium Chloride

Sterilize by filtering through a 0,2 µm filter and store at 4º.

4.2. 10% FBS MEM:F12 (1:1)

For a final volume of 1L:

- 4,805 g of MEM (Gibco, Invitrogen);
- 5,315 g of F12 (Gibco, Invitrogen);
- 1,5 g of $NaHCO_3$ (Sigma);
- 0,055 g of Sodium pyruvate (Sigma);
- 10 mL of 1% antibiotic/antimycotic (AA) mix (Gibco, Invitrogen);
- 100 mL of 10% FBS (Gibco, Invitrogen);
- 2,5 mL of L-glutamine (200 mM stock solution);

Dissolve in dH_2O, adjust the pH to 7,2 / 7,3 and adjust the volume to 1L with dH_2O.

4.3. Freezing medium

- Growth medium (MEM:F12) – 7mL;
- FBS (10%) – 2mL
- DMSO (5-20%) – 1mL

4.4. 4% Paraformaldehyde

For a final volume of 100 mL, add 4g of paraformaldehyde to 25 mL of dH_2O. Dissolve by heating the mixture at 58ºC while stirring. Add 1-2 drops of 1 M NaOH to clarify the solution and filter (0,2 µm filter). Add 50mL of 2x PBS and adjust the volume to 100 mL with dH_2O.